SYNTHESIS AND EVALUATION OF BOTH PHOSPHONIC- AND BISPHOSPHONIC ACID FUNCTIONALIZED MONOMERS FOR LONGER-LASTING DENTAL FILLINGS

by

Türkan Gençoğlu

B.S., Chemistry, Boğaziçi University, 2016

Submitted to the Institute for Graduate Studies in

Science and Engineering in partial fulfillment of

the requirements for the degree of

Master of Science

Graduate Program in Chemistry

Boğaziçi University

2017

SYNTHESIS AND EVALUATION OF BOTH PHOSPHONIC- AND BISPHOSPHONIC ACID FUNCTIONALIZED MONOMERS FOR LONGER-LASTING DENTAL FILLINGS

APPROVED BY:

Prof. Duygu Avcı Semiz (Thesis Supervisor)	.....
Assist. Prof. Fırat İlker	.....
Assist. Prof. Funda Oğuz	.....

DATE OF APPROVAL: ……..

ACKNOWLEDGEMENTS

This research has been financially supported by The Scientific and Technological Research Council of Turkey (TÜBİTAK) [215Z060].

I would like to thank Prof. Duygu Avcı Semiz for her support and guidance throughout the research.

ABSTRACT

SYNTHESIS AND EVALUATION OF BOTH PHOSPHONIC- AND BISPHOSPHONIC ACID FUNCTIONALIZED MONOMERS FOR LONGER-LASTING DENTAL FILLINGS

It is possible to increase the lifetime of dental restorations by improving the performaces of 'self-etching' adhesives and/or dental composites. In this work, the first monomers containing both phosphonate and bisphosphonate or phosphonic and bisphosphonic acid functionalities were synthesized for stronger interaction with tooth structure; and their properties were analyzed. For the synthesis of monomers, two amines (A1 and A2) having both phosphonate and bisphosphonate functionalities were synthesized. Reaction of these amines with with acryloyl chloride gave two novel acrylamide monomers (AAm-1 and AAm-2) with both phosphonate and bisphosphonate. It was impossible to synthesize acid derivatives of these monomers due to disappearance of double bonds; but their copolymers with poly(ethylene glycol)methyl ether methacrylate containing both phosphonic and bisphosphonic acid were obtained. Reaction of the same amines with 2-isocyanatoethyl methacrylate gave two novel methacrylate monomers (MA-A1 and MA-A2) with both phosphonate and bisphosphonate. By deprotection of phosphonate and bisphosphonate ester groups of MA-A1 and MA-A2, two novel methacrylates (MA-A1-Ac and MA-A2-Ac) with both phosphonic and bisphosphonic acid were synthesized. Copolymerization reactivities of the synthesized monomers with 2-hydroxyethyl methacrylate (HEMA) and bisphenol A glycidyl methacrylate (Bis-GMA)/triethyleneglycol dimethacrylate (TEGDMA) mixtures were investigated with real-time FTIR or photo differential scanning calorimetry. The acid monomers were found to have mild self-etching (pH = 1.65 ve 1.66) primer properties. Scanning electron microscopy (SEM) revealed that they can partially remove the smear layer on dentin and cause demineralization. X-Ray Diffractometer (XRD), FTIR and X-ray photoelectron spectroscopy (XPS) analyses of MA-A2-Ac-treated HAP particles (representative of tooth) showed formation of stable monomer-Ca salts. The acid monomers were found to be suitable for use in dental adhesives due to their solubilities in water, etching abilities, high copolymerization reactivities and their strong interaction with HAP. Addition of these monomers to dental composites is expected to improve longetivity of dental restorations.

ÖZET

UZUN ÖMÜRLÜ DİŞ DOLGULARI İÇİN FOSFONİK VE BİSFOSFONİK ASİT İÇEREN MONOMERLERİN SENTEZİ VE DEĞERLENDİRİLMESİ

‘Self-etching’ (kendinden aşındırmalı) diş yapıştırıcılarının ve/veya diş kompozitlerinin performanslarının arttırılarak diş restorasyonlarının kullanım ömürlerinin uzatılması mümkündür. Bu çalışmada, yapılarında diş dokusu ile daha iyi bağlanmak üzere fosfonat ve bisfosfonat ya da fosfonik ve bisfosfonik asit gruplarını birlikte içeren ilk monomerler sentezlenerek özellikleri incelenmiştir. Monomerlerin sentezleri için yapılarında fosfonat ve bisfosfonat gruplarını birlikte içeren iki amin (A1 ve A2) sentezlenmiştir. Bu aminlerin akriloil klorür ile tepkimelerinden fosfonat ve bisfosfonat gruplarını birlikte içeren iki yeni akrilamid monomeri (AAm-A1 ve AAm-A2) sentezlenmiştir. Bu monomerlerin asit türevlerinin sentezleri çift bağların kaybolması dolayısıyla gerçekleştirilememiş ancak poli(etilen glikol)metil eter metakrilat ile fosfonik ve bisfosfonik asit grupları taşıyan kopolimerleri sentezlenmiştir. Aynı aminlerin 2-izosiyanatoetilmetakrilat ile tepkimeleri fosfonat ve bisfosfonat gruplarını birlikte içeren iki yeni metakrilat (MA-A1 ve MA-A2) vermiştir. MA-A1 ve MA-A2’nin fosfonat ve bisfosfonat ester gruplarının deproteksiyonuyla fosfonik ve bisfosfonik asit gruplarını birlikte içeren iki yeni metakrilat (MA-A1-Ac ve MA-A2-Ac) sentezlenmiştir. Sentezlenen monomerlerin ticari diş monomerlerinden 2-hidroksietil metakrilat (HEMA) ve bisfenol A glisidil metakrilat (Bis-GMA)/trietilenglikol dimetakrilat (TEGDMA) karışımları ile kopolimerleşme reaktiflikleri gerçek zamanlı FTIR ya da foto-diferansiyel taramalı kalorimetre ile incelenmiştir. Asit monomerler, orta kuvvetli “self-etching” (pH = 1.65 ve 1.66) primer özelliğine sahip bulunmuş, taramalı elektron mikroskopu (SEM) incelemesinde dentin üzerindeki “smear” tabakasını kısmen yok edip demineralizasyon sağladıkları gözlenmiştir. Dişi temsilen bu monomerlerden MA-A2-Ac ile muamele edilmiş HAP partiküllerinin X-ışını difraktometre (XRD), FTIR ve X-ışını fotoelektron spektroskopi (XPS) analizleri, monomer-HAP etkileşimi sonucu kararlı monomer-Ca tuzlarının oluştuğunu (ticari monomerlerden 10-metakriloiloksidesil dihidrojen fosfat ile benzer) göstermiştir. Asit monomerlerinin diş yapıştırıcılarında kullanıma uygun oldukları bulunmuştur.

TABLE OF CONTENTS

ACKNOWLEDGEMENTS.....iii

ABSTRACT.....iv

ÖZET.....v

LIST OF FIGURES.....ix

LIST OF TABLES.....xii

LIST OF ACRONYMS/ABBREVIATIONS.....xiii

1. INTRODUCTION.....1

2. MATERIALS AND METHODS.....10

2.1. Materials.....10

2.2. Characterization.....10

2.3. Synthesis of Starting Materials.....11

2.3.1. Synthesis of Diethyl (2-aminoethyl)phosphonate.....11

2.3.2. Synthesis of Diethyl (6-aminohexyl)phosphonate.....11

2.3.3. Synthesis of Tetraethyl Vinylidene Bisphosphonate.....12

2.3.4. Synthesis of Amines Containing Both Phosphonate and Bisphosphonate (A1 and A2).....13

2.3.4.1. A1.....13

2.3.4.2. A2.....13

2.4. Synthesis of Monomers.....13

2.4.1. Synthesis of Acrylamides Containing Both Phosphonate and Bisphosphonate.....13

2.4.1.1. AAm-A1.....14

2.4.1.2. AAm-A2.....14

2.4.2. Synthesis of Acrylamides Containing Both Phosphonic and Bisphosphonic Acid.....14

2.4.3. Synthesis of Methacrylates Containing Both Phosphonate and Bisphosphonate.....15

2.4.3.1. MA-A1.....15

2.4.3.2. MA-A2.....15

2.4.4. Synthesis of Methacrylates Containing Both Phosphonic and Bisphosphonic Acid.....16

2.4.4.1. MA-A1-Ac.....16

2.4.4.2. MA-A2-Ac.....16

2.5. Etching Performances of Monomers.....17

2.6. HAP Interaction of Monomers.....17

2.6.1. FTIR.....17

2.6.2. XRD.....18

2.6.3. XPS.....18

2.7. Photopolymerization.....18

2.8. *In vitro* Cytotoxicity Assay.....19

2.9. Thermal Copolymerization.....20

2.9.1. Synthesis of AAm-A2-co-PEGMA copolymer.....20

2.9.1.1. AAm-A2-co-PEGMA (50:50 mol%).....20

2.9.1.2. AAm-A2-co-PEGMA (20:80 mol%)……..……..…...…...20

2.9.2. Deprotection of AAm-A2-co-PEGMA copolymer…..…..…...…..…20

3. RESULTS……...….....…...…..21

3.1. Synthesis and Characterization of Monomers……...….....…….....21

3.2. Acidity and HAP Interactions of Monomers…….....….....…….…..32

3.3. Photopolymerization.……..…….....…..…….....…..…...35

3.4. *In vitro* Cytotoxicity Assay….....…….....…..…....…..…...43

3.5. Thermal Polymerization…….……....……...…....…43

4. DISCUSSION & CONCLUSION…….…….…….…….....48

5. REFERENCES…….…….…….…..……...…...…51

LIST OF FIGURES

Figure 1.1. The methacrylate monomers used in the resin matrix of dental composites…...2

Figure 1.2. General strucure of adhesive monomers…….....……..2

Figure 1.3. Adhesion-Decalcification Concept…….…….3

Figure 1.4. TEM images of dentin-adhesive interfaces……....…….4

Figure 1.5. Components of Self-Etching Enamel-Dentin Adhesives…….……...……5

Figure 1.6. XPS spectra of untreated HAP, HAP treated with 4-MET, with 10-MDP, and with phenyl P…….…….…….…5

Figure 1.7. XRD spectrum of dentin treated with monomers…….....….…..6

Figure 1.8. Monomer structures and SBS results…….…….....…….6

Figure 1.9. Photopolymerization results…….….....……...7

Figure 1.10. General structures of Pyrophosphate and Bisphosphonate……....7

Figure 1.11. Bisphosphonate possessing self-etching compounds synthesized by our group……..…….……8

Figure 1.12. Structures and Names of the Synthesized Novel Monomers…….……9

Figure 3.1. Synthesis of starting materials of A1 and A2…….…..…….22

Figure 3.2. Synthesis of A1, A2, AAm-A1, AAm-A2, MA-A1, MA-A2, MA-A1-Ac, and MA-A2-Ac……..……...……...23

Figure 3.3. FTIR and ^{1}H NMR spectra of A1……..…….……...24

Figure 3.4. FTIR and ^{1}H NMR spectra of A2……..…….……...25

Figure 3.5. FTIR and ^{1}H NMR spectra of AAm-A1……..…….…….26

Figure 3.6. FTIR and ^{1}H NMR spectra of AAm-A2……....…….……..27

Figure 3.7. FTIR and ^{1}H NMR spectra of MA-A1..…….……...28

Figure 3.8. FTIR and ^{1}H NMR spectra of MA-A2……..…….……...29

Figure 3.9. ^{13}C NMR spectra of MA-A1 and MA-A2……..……..30

Figure 3.10. FTIR and ^{1}H NMR spectra of MA-A1-Ac…….…….31

Figure 3.11. ^{1}H NMR spectrum of MA-A2-Ac…….……...……..32

Figure 3.12. SEM image of dentin etched with 20 w% MA-A2-Ac containing EtOH/H_2O (v/v) solution, 1000 x (left) vs 10000 x (right)……..……..……33

Figure 3.13. FTIR spectra of EtOH/H_2O phase of MA-A1-Ac treated HAP (top spectra) and MA-A1-Ac (bottom spectra)……...……...……...…...33

Figure 3.14 FTIR spectra of HAP (bottom spectra) and MA-A2-Ac treated HAP (top spectra)……..…….…….34

Figure 3.15. XPS spectrum of HAP (bottom spectra), HAP treated with MA-A2-Ac (middle spectra), and MDP treated HAP (top spectra)…..……..34

Figure 3.16. XRD spectra of MA-A2-Ac treated HAP……...35

Figure 3.17. Conversion vs time plot of HEMA:AAm-A1 and HEMA:AAm-A2 mixtures at different temperatures……..……..….36

Figure 3.18. Conversion vs time plot of Bis-GMA:TEGDMA:AAm-A1 and Bis-GMA:TEGDMA:AAm-A2 mixtures at different temperatures……....37

Figure 3.19. R_p vs time plot for Bis-GMA:TEGDMA:MA-A1/MA-A2 mixtures at 37 °C.....39

Figure 3.20. Conversion vs time plot for Bis-GMA:TEGDMA:MA-A1/MA-A2 mixtures at 37 °C…….……...…39

Figure 3.21. R_p vs time plot for HEMA:MA-A1/MA-A2 mixtures at 37°C.....…40

Figure 3.22. Conversion vs time plot for HEMA:MA-A1/MA-A2 mixtures at 37 °C...…40

Figure 3.23. R_p vs time plot for HEMA, HEMA:MA-A2-Ac, Bis-GMA:TEGDMA, and Bis-GMA:TEGDMA:MA-A2-Ac mixtures at 37 °C (initiator:BAPO).....41

Figure 3.24. Conversion vs time plot for HEMA, HEMA:MA-A2-Ac, Bis-GMA: TEGDMA and Bis-GMA:TEGDMA:MA-A2-Ac mixtures at 37 °C (initiator:BAPO)…….……...41

Figure 3.25. R_p vs time plot for HEMA, HEMA:MA-A2-Ac, and HEMA:water:MA-A2-Ac mixtures at 37 °C (initiator: BAPO)…….....…..42

Figure 3.26. Conversion vs time plot for HEMA, HEMA:MA-A2-Ac, and HEMA: water:MA-A2-Ac mixture at 37 °C (initiator: BAPO)….……..…....42

Figure 3.27. Cell viability plot of MA-A2 and MA-A2-Ac…….....……....43

Figure 3.28. ^{1}H NMR spectrum of PEGMA:AAm-A2 (50:50 mol% in feed) copolymer...44

Figure 3.29. ^{1}H NMR spectrum of PEGMA:AAm-A2 (80:20 mol% in feed) copolymer...45

Figure 3.30. FTIR spectrum of PEGMA:AAm-A2 (80:20 mol% in feed) copolymer…....45

Figure 3. 31. ^{1}H NMR spectrum of deprotected PEGMA:AAm-A2 (80:20 mol% in feed) copolymer……..46

Figure 3.32. FTIR spectrum of deprotected PEGMA:AAm-A2 (80:20 mol% in feed) copolymer……..……....46

LIST OF TABLES

Table 3.1. Solubilities of amines and monomers in different solvents……..…….47

LIST OF ACRONYMS/ABBREVIATIONS

AIBN	2,2′-azobis(2-methylpropionitrile)
BAPO	Phenylbis(2,4,6-trimethylbenzoyl)-phosphine oxide
Bis-GMA	Bisphenol A-glycidyl methacrylate
BP	Bisphosphonate
DMPA	2,2'-Dimethoxy-2-phenyl acetophenone
FT-IR	Fourier Transform Infrared Spectroscopy
HAP	Hydroxyapatite
HEMA	2-Hydroxyethyl methacrylate
IEM	2-isocyanatoethyl methacrylate
MDP	10-Methacryloyloxydecyl dihydrogen phosphate
MTT	Thiazolyl blue tetrazolium bromide
NMR	Nuclear Magnetic Resonance spectroscopy
PBS	Phosphate Buffered Saline
PEGMA	Poly(ethylene glycol) methyl ether methacrylate
p-TsOH	Para-toluene sulfonic acid
SBS	Shear Bond Strength
SEM	Scanning Electron Microscope
TEGDMA	Triethylene glycol dimethacrylate
TMSBr	Trimethylsilyl Bromide
XRD	X-ray Diffraction
XPS	X-ray Photoelectron Spectroscopy

1. INTRODUCTION

Phosphonates or phosphonic acids are the important members of organophosphorus compounds. Their importance stems from their properties such as metal binding, biocompatibility, stability in harsh conditions, and water solubility. These properties allow phosphonates to be used in many different application areas. Any area requiring coordinating agent can benefit from phosphonates. In anionic form, they can bind to any metal through oxygens that are singly bonded to phosphorus. Anti-corrosion agents, recovery of metal ions, ion-exchange resins need materials having affinity toward metal ions. Therefore, phosphonates are successful agents in these fields [1-6]. They possess the chemically, hydrolytically and thermally stable C-P bond. When metal ion affinity is combined with water solubility and hydrolytic stability, a new gate opens for phosphonates: water treatment. Water should be treated to eliminate metal ions because heavy and high concentrations of metal ions are harmful for living organisms and environment, thus phosphonates are widely used in this field [7,8]. Furthermore, radical scavenging ability and stability of phosphonates in harsh conditions such as high temperature lead them to be used as flame retardants [9,10]. They are also beneficial compounds for biomedical applications such as implant coating [11,12], drug delivery [13,14] and dental restorations [15] when their biocompatibility is combined with metal binding ability. There are numerous application fields for phosphonates as discussed, but we specifically focused on dental restorations in this study.

In the past, amalgam fillings were applied to decayed or fractured teeth for years. However, because of their metal content, medical concerns rose. Besides, they are not tooth-colored, so they don't look aesthetic. These reasons led them to be replaced by dental restorative composites. Dental composites are biomaterials which consist of resin matrix, fillers, coupling agents, initiators and inhibitors. The resin matrix consists of methacrylate and dimethacrylates such as HEMA, Bis-GMA, and TEGDMA etc. (Figure 1.1). Composites have many ingredients, but none of them has strong interaction with tooth structure. Weak interaction leads to shorter lifetime for fillings. To improve the interaction, thus the lifetime, an additional material is used. The additional materials are called 'dental adhesives'. Adhesive monomer structure is presented in Figure 1.2 [16]. Their job is to

form a connection between the composite resin and tooth tissue (enamel and dentin). Hydroxyapatite [HAP,$Ca_{10}(PO_4)_6(OH)_2$] is the basic mineral structure of tooth. Enamel and dentin rich in HAP, so they are rich in calcium. Adhesive monomers connect tooth and composite resin through the following mechanism: they chelate with calcium ions in enamel and dentin through acidic functional group, and they also copolymerize with the resin matrix via the polymerizable group simultaneously.

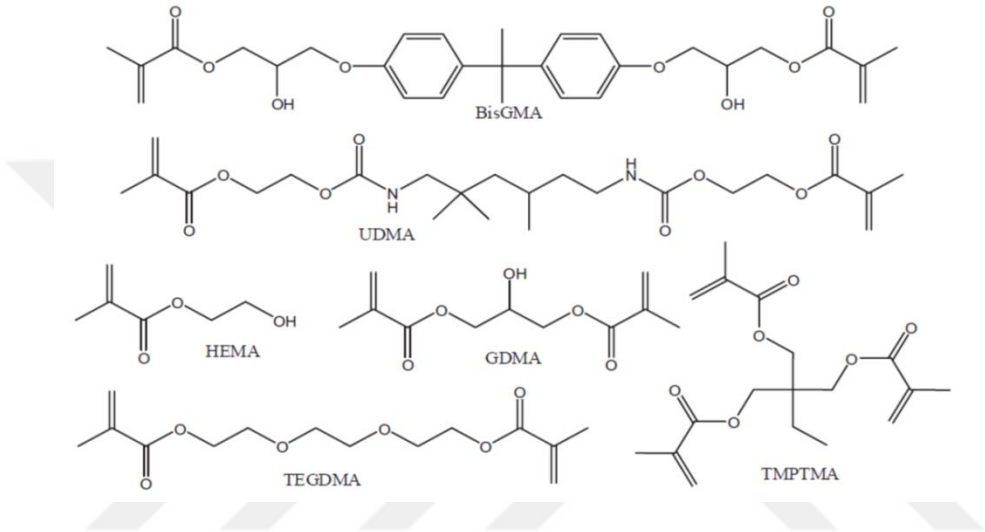

Figure 1.1. The methacrylate monomers used in the resin matrix of dental composites

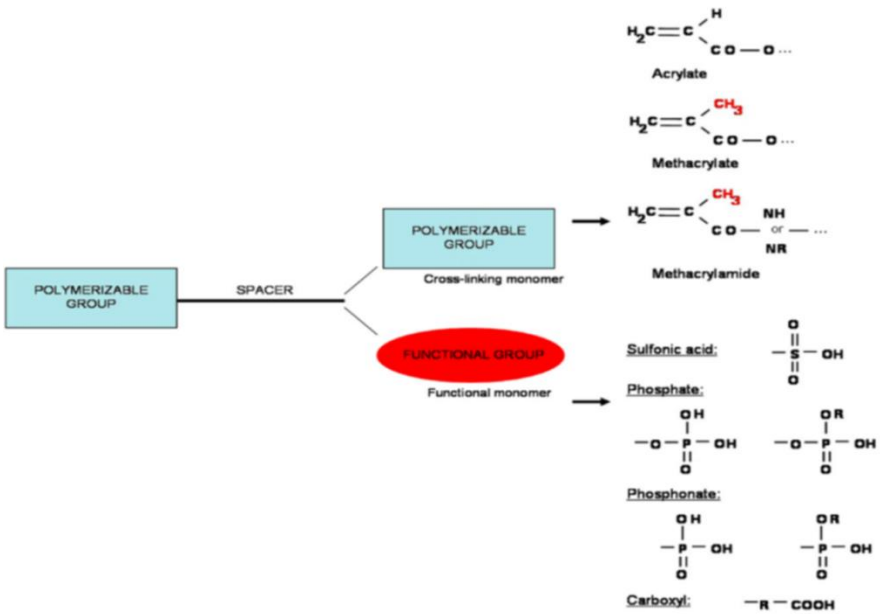

Figure 1.2. Generel structure of adhesive monomers [16]

Before applying filling materials, tooth is subjected to a certain procedure. This process creates a layer (smear layer) which blocks the dentinal tubules. Eventually, the filling materials cannot go into the tubules, so they cannot bind strongly to tooth. Hence the smear layer should be removed before applying restoratives. The removal process is called 'etching'. Acidic compounds such as phosphoric acid are used as etchants [17]. However, phosphoric acid almost completely demineralizes dentin. Complete demineralization decreases the strength of adhesive's adhesion to tooth. Therefore new etchants needed to be found. It was considered that adhesive monomers could be utilized as etchant since they have acidic functionality such as carboxylic or phosphonic acid (Figure 1.2). This idea has established a new class of materials: self-etching adhesives. They are designed to form a connection between dental restoratives and enamel or dentin [18-22]. Firstly, they interact with HAP by the 'Adhesion-Decalcification Mechanism' [22,23] (Figure 1.3). Bond formation to dental tissues is related to acidic monomer structure [24-27]. The acidic group in self-etching adhesive monomer is ionized by water, forms an ionic bond with calcium, OH^- and PO_4^{3-} ions are removed (etching). This process removes the smear layer and opens up the dentinal tubules. Then, it replaces the removed ions and forms a complex with Ca. If the complex is water-soluble HAP is decalcified, the complex is washed away and adhesive monomer cannot penetrate into tubules. If the complex is stable and not water-soluble, HAP is partially decalcified. The monomer

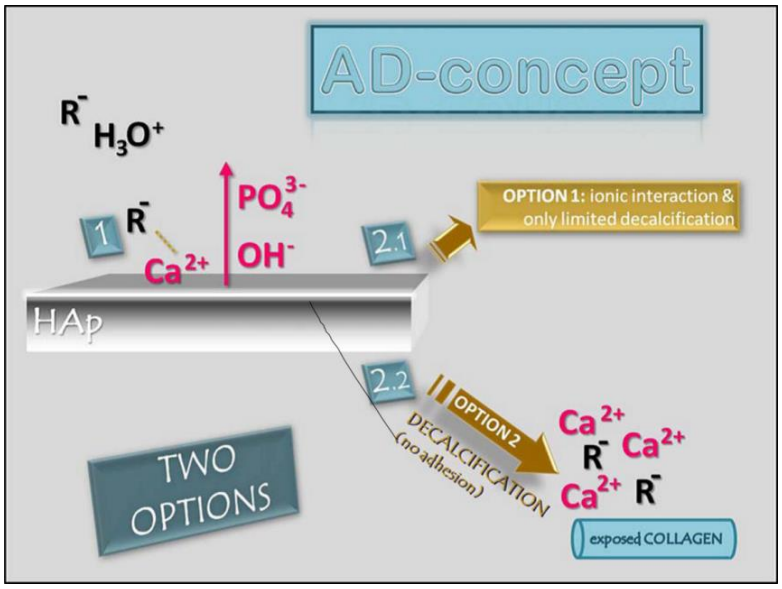

Figure 1.3. Adhesion-Decalcification Concept [22]

infiltrates into the tubules, forms a hybrid layer with collagen [28]. It also polymerizes with dental restoratives with its polymerizable group via photopolymerization. When the restorative is attached to monomer, it would be also incorporated into the hybrid layer. The hybrid layer's thickness is dependent on pH. Self-etching adhesives are classified into 3 categories based on their pH: ultra-mild (pH > 2.5), mild (pH≈2), and strong (pH≤1) self-etching adhesives. Ultra-mild, mild, and strong self-etching adhesives form 300 nm, 0.5-1 μm, 4 μm hybrid layer, respectively (Figure 1.4) [22].

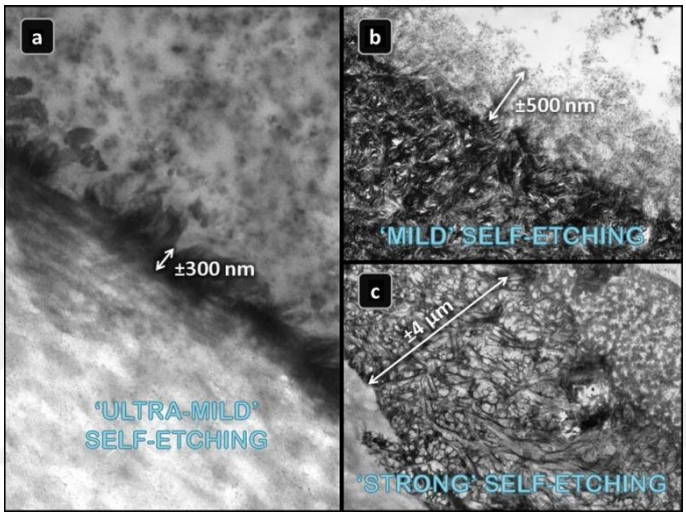

Figure 1.4. TEM images of dentin-adhesive interfaces [22]

It is important to develop new acidic monomers for enhancing the effectiveness of dental restorations. Such a monomer should fulfill the following requirements: (i) strong binding to dental tissues; (ii) solubility in the adhesive mixture; (iii) high homo- and copolymerization rate with comonomers; (iv) low volume shrinkage; (v) resistance to hydrolyis; (vi) ability to etch enamel and dentin; (vii) solubility in ethanol and water; (viii) compatibility with dental tissues; (ix) minimum water absorption and no swelling of its polymer.

Self-etching adhesives involve acidic groups such as carboxylic, phosphoric or phosphonic acids (Figure 1.2). Commercial 'self-etching' adhesive systems have combined ingredients of restorative compounds with adhesive monomers. They include 'self-etching' adhesives [2-methacryloyloxyethyl dihydrogen phosphate (MEP), 10-methacryloyloxydecyl dihydrogen phosphate (MDP), 4-methacryloyloxyethyl trimellitic acid (4-MET) etc.], crosslinking monomers [TEGDMA, Bis-GMA etc.], monofunctional

comonomers (e.g. HEMA), photoinitiators, and filling materials (Figure 1.5) [29]. The interaction between HAP and MDP, 4-MET, and phenyl-P was characterized in the literature [30,31]. The self-etching adhesives partially demineralized dentin, and formed a hybrid layer. The interaction was further analyzed by XPS (Figure 1.6). Based on the changes in C 1s peak, it was concluded that these self-etch adhesives adhered on HAP.

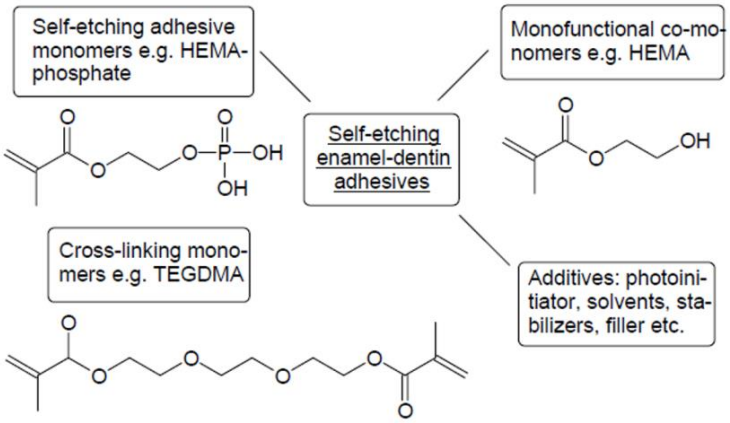

Figure 1.5. Components of Self-Etching Enamel-Dentin Adhesives [29]

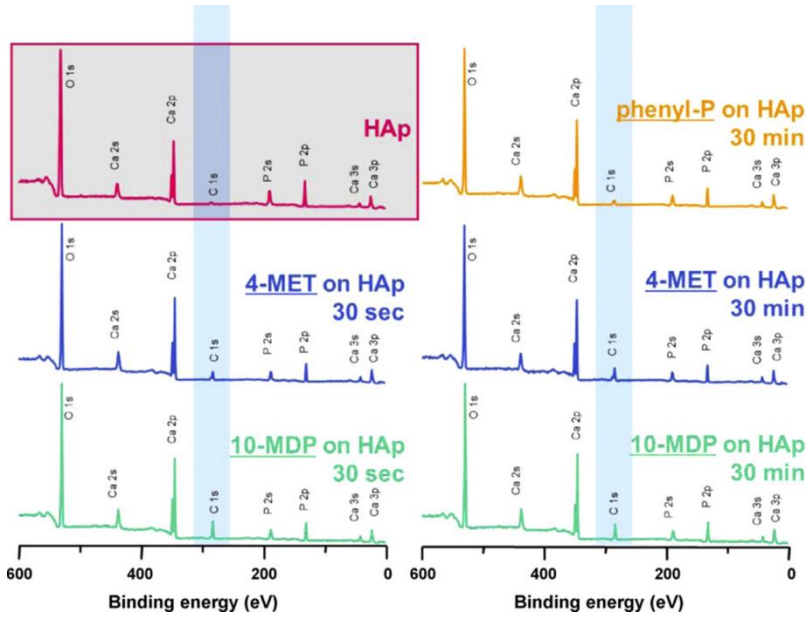

Figure 1.6. XPS spectra of untreated HAP, HAP treated with 4-MET, with 10-MDP, and with phenyl-P [31]

Phosphonic and phosphoric acid containing monomers are present in literature [32-51]. Properties of 3 monomers possessing phosphonate was analyzed [27,52]. It was found out that structures of the monomers affected their bonding to dentin. As presented in Figure 1.7, HAEPA, most hydrophilic one, didn't form a stable interaction with dentin whereas MAEPA and EAEPA - more hydrophobic - formed stable, insoluble calcium salt [52]. Hydrophilicity of the monomers determined their bonding to dentin.

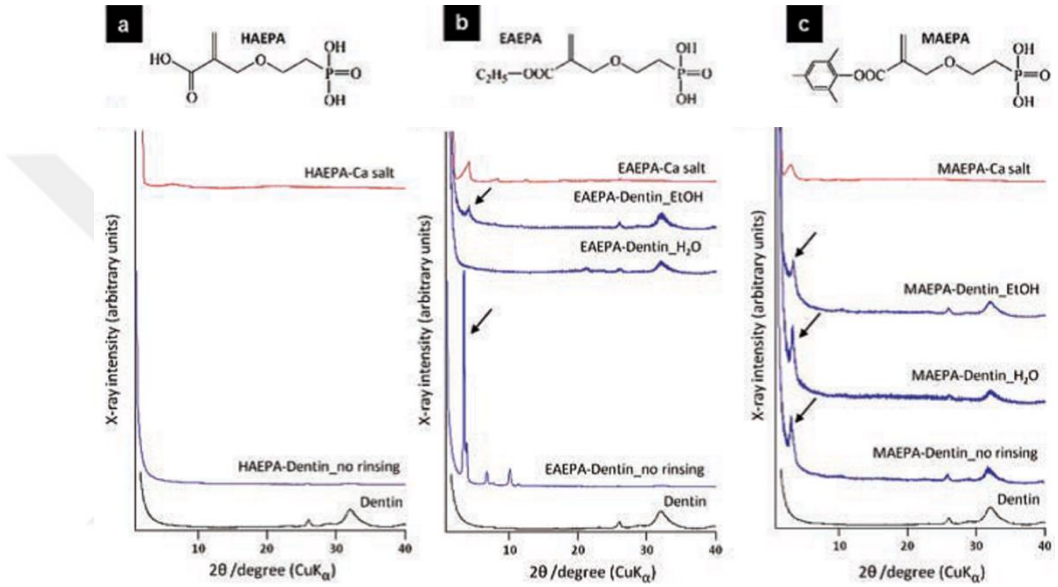

Figure 1.7. XRD spectrum of dentin treated with monomers [52]

Catel *et al*. [53] synthesized compounds having both phosphonate and phosphate functionalities. Figure 1.8 depicts that these synhesized monomers have higher shear bond strength (SBS) than MDP (commercial adhesive). Higher SBS was attributed to improved chelating ability caused by presence of two acidic groups.

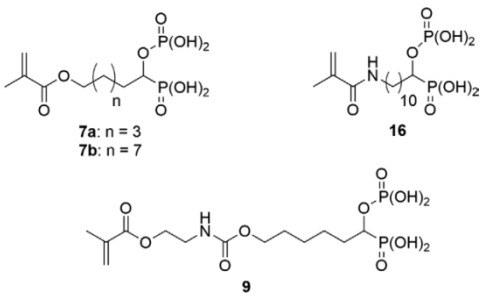

SEA	Acidic monomer	Dentin SBS (MPa)	Enamel SBS (MPa)
1	7a	37.3 ± 5.1	29.1 ± 4.5
2	7b	36.5 ± 4.1	25.8 ± 2.8
3	9	38.5 ± 3.8	29.8 ± 3.0
4	16	33.8 ± 3.7	27.9 ± 2.9
5	MDP	27.7 ± 4.8	22.6 ± 4.0
6	MDPA	22.0 ± 3.3	16.4 ± 2.8

Figure 1.8. Monomer structures and SBS results [53]

Acrylamide containing adhesives were developed to improve the hydrolytic stability and durability of adhesives [33,54,55]. Besse *et al*. [56] synthesized acrylamide containing phosphonate and phosphonic acid compounds and analyzed their photopolymerization reactivity by copolymerizing them with DEBAAP (bis-acrylamide). Results showed that when copolymerized with 1 or 2, max. polymerization rate increased (Figure 1.9). The increase was observed more with phosphonic acid monomer 1.

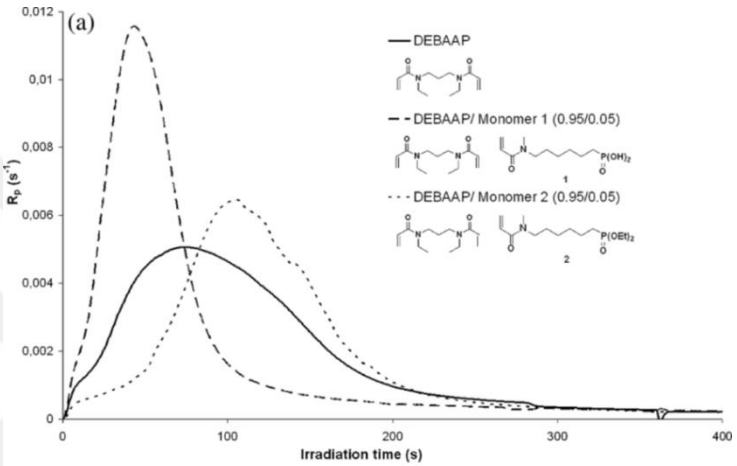

Figure 1.9. Photopolymerization results [56]

Bisphosphonic acids (BP, referred as bisphosphonate in literature) are synthetic analogues of inorganic pyrophosphate, resistant to enzymatic hydrolysis and have ability to bind strongly to bone surface (Figure 1.10) [57-60]. Strong interaction with HAP stems from having two phosphonate groups $\{(HO)_2(O)P\text{-}C\text{-}P(O)\text{-}(OH)_2\}$. Besides, BPs suppress enzymes (metalloproteinases) responsible for collagen network degradation.



Pyrophosphate Bisphosphonic Acid

Figure 1.10. General structures of Pyrophosphate and Bisphosphonate

Bisphosphonic acid monomers have been synhesized to be used in self-etching adhesives currently [61-65]. They also have been synthesized by our group (Figure 1.11) [66,67].

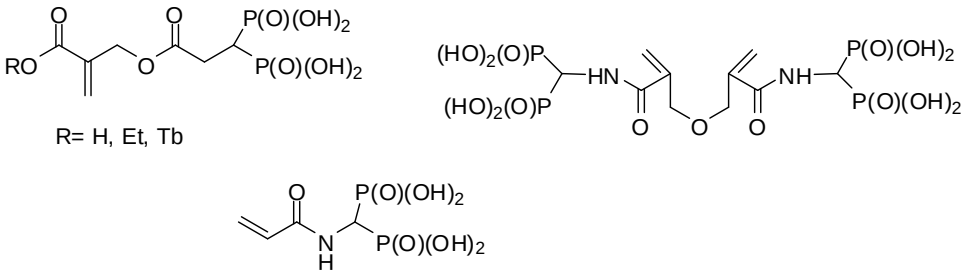

Figure 1.11. Bisphosphonate possessing self-etching compounds synthesized by our group

In this thesis, the first monomers which contain both phosphonate/bisphosphonate or phosphonic/bisphosphonic acid functionalities were synthesized to improve self-etching dental adhesive' and/or dental composites' performances via enhanced HAP interaction and by extending their shelf-life. Two of these are acrylamide monomers containing both phosphonate and bisphosphonate (AAm-A1 and AAm-A2) (Figure 1.12). A dealkylation reaction for converting phosphonate and bisphosphonate into phosphonic and bisphosphonic acid was not successful. Four of the novel monomers are methacrylate monomers (MA-A1, MA-A2, MA-A1-Ac, MA-A2-Ac) featuring both phosphonate and bisphosphonate or both phosphonic and bisphosphonic acid functionalities (Figure 1.12). The potential to use the monomers in dental composites and adhesives was investigated; pH, solubility, homo- and copolymerization reactivities with other dental monomers [2-hydroxyethyl methacrylate (HEMA), and bisphenol A glycidyl methacrylate (Bis-GMA)/ triethyleneglycol dimethacrylate (TEGDMA) mixture] were examined by either real-time FTIR or photo-differential scanning calorimetry. One of the acidic monomers (MA-A2-Ac) was analyzed by SEM to find out its 'etching' potential, and also analyzed by FTIR, XRD, and XPS to observe its adhesive properties.

The AAm-A2 monomer was copolymerized with poly(ethylene glycol)methyl ether methacrylate (PEGMA, M_n = 950). The phosphonate and bisphosphonate groups of the copolymer were deprotected to convert them into phosphonic and bisphosphonic acid. The acidic copolymer is expected to have ability to biomineralize HAP or to target bone.

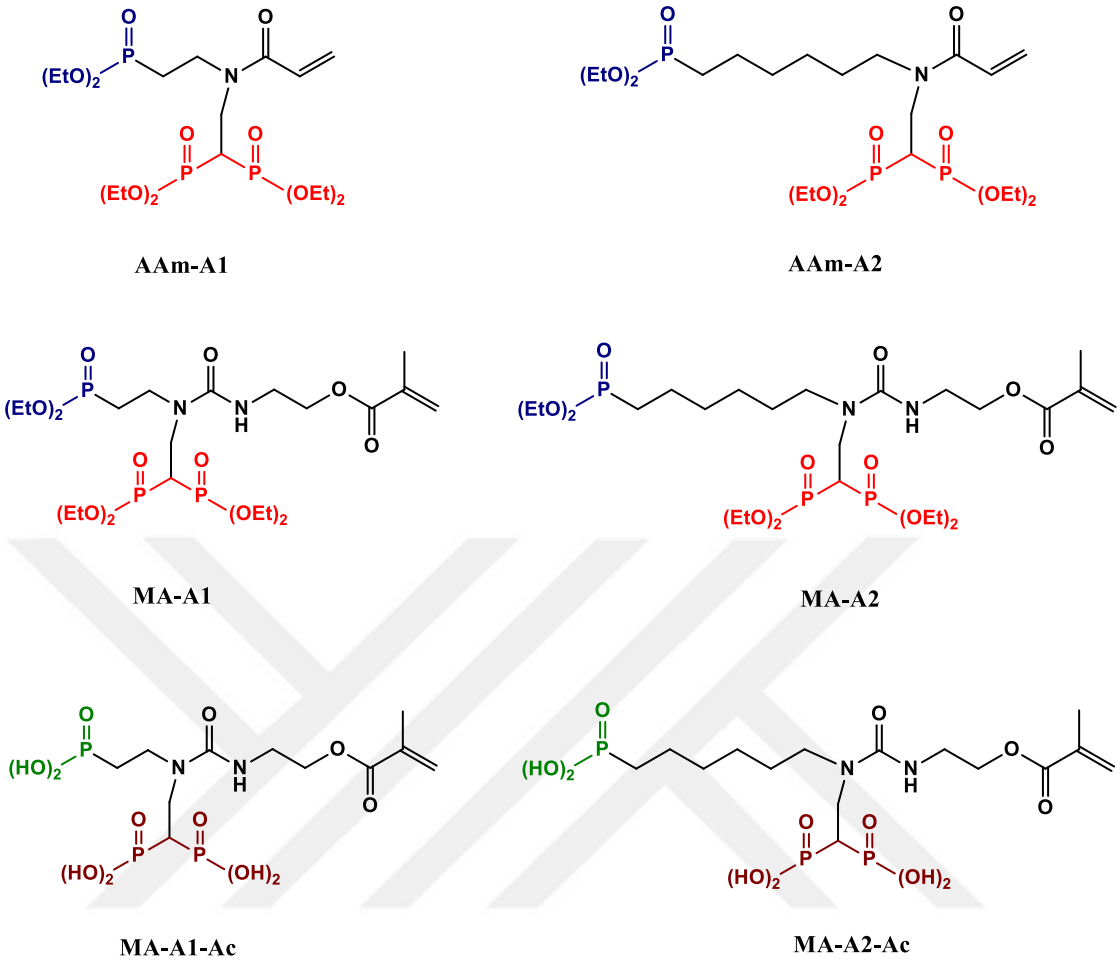

Figure 1.12. Structures and Names of the Synthesized Novel Monomers

2. MATERIALS AND METHODS

2.1. Materials

Acryloyl chloride, triethyl amine (TEA), diethyl amine, diethyl vinylphosphonate, 2-isocyanatoethyl methacrylate (IEM), 2-hydroxyethyl methacrylate (HEMA), 1,6-dibromo hexane, trimethylsilyl bromide (TMSBr), triethyl phosphite, potassium phtalimide, hydrazine monohydrate, diethyl phosphite, paraformaldehyde, tetraethyl methylene diphosphonate, bisphenol A glycidyl methacrylate (Bis-GMA), triethylene glycol dimethacrylate (TEGDMA), para-toluene sulfonic acid (pTsOH), poly(ethylene glycol)methyl ether methacrylate (PEGMA, M_n = 950), 2,2-dimethoxy-2-phenylacetophenone (DMPA), phenylbis(2,4,6-trimethylbenzoyl)-phosphine oxide (BAPO), 2,2′-azobis(2-methylpropionitrile) (AIBN), and the other chemicals and solvents were supplied from Aldrich Chemical Co. and used without purification. 10-methacryloyloxydecyl diphosphate (MDP) was supplied by Ivoclar Vivadent AG.

2.2. Characterization

^{1}H-, ^{13}C NMR spectra were recorded on a Varian Gemini (400 MHz) spectrometer with deuterated chloroform ($CDCl_3$) or methanol (MeOD) as solvent, and tetramethylsilane as an internal standard. Fourier transform infrared (FTIR) spectra of monomers were recorded with a Nicolet 6700, Thermo spectrometer. Combi Flash Companion Teledyne ISCO Flash Chromatography with C18 reverse phase column was used for purification of monomers. XRD patterns of HAP particles treated with the monomers were recorded using powders by coupled θ-2θ XRD (D8 Advance; Bruker, Karlsruhe), with a CuK_α source (λ=1.5418 Å) at operating parameters of 40 kV and 40 mA and with step size of 0.01°. XPS studies were carried on a Thermo Scientific K-Alpha X-ray Photoelectron Spectrometer. SEM images of monomer treated enamel and dentin samples were recorded by SEM (FEI-Philips XL30).

2.3. Synthesis of Starting Materials

2.3.1. Synthesis of Diethyl (2-aminoethyl)phosphonate

It was synthesized according to a literature procedure [68]. Diethyl vinylphosphonate (1.64 g, 10 mmol) was added to ice-cold NH_4OH solution (32%) dropwise, and the mixture was stirred at room temperature for 24 hours. Then the reaction mixture was extracted with chloroform (4 x 15 mL). The organic phase was dried over Na_2SO_4, filtered off, and chloroform was evaporated. The residue was purified by vacuum distillation to give the pure product as a colorless liquid in 30% yield.

FTIR (ATR): 953, 1022 (P-O), 1231 (P=O), 2904 (C-H), 3376 (NH) cm^{-1}.

^{1}H-NMR (400 MHz, $CDCl_3$, *δ)*: 1.32 (6H, OCH_2CH_3), 2.03 (2H, CH_2-P), 2.87 (2H, CH_2NH_2), 4.11 (4H, OCH_2CH_3) ppm.

2.3.2. Synthesis of Diethyl (6-aminohexyl)phosphonate

It was synthesized in three steps according to the literature procedures [69-71]. Potassium phthalimide (0.74 g, 4 mmol) and 1,6-dibromohexane (1.85 mL, 12 mmol) were stirred at 150 °C for 12 hours. Then chloroform was added and precipitate was filtered. After removel of the solvent, petroleum ether preheated to 50 °C was added and the precipitate formed was filtered. The remaining solution was kept in the refrigirator overnight to precipitate N-(6-bromohexyl)phtalimide crystals (45% yield).

N-(6-bromohexyl)phtalimide (0.89 g, 2.9 mmol) was added to triethyl phosphite (2.21 g, 13.3 mmol), and the mixture was refluxed at 150 °C for 12 hours. Excess triethyl phosphite was distilled off under reduced pressure (3 mmHg) at 60 °C to give diethyl 6-phthalimidohexylphosphonate as a yellow liquid in 70% yield.

To ethanol (44.4 mL) solution of diethyl 6-phthalimidohexylphosphonate (0.88 g, 2.4 mmol) hydrazine monohydrate (1.2 g, 24 mmol) was added and the solution was stirred at room temperature for 12 hours. The precipitate was filtered and EtOH was removed under reduced pressure. To the crude product, dichloromethane (2 mL) and distilled water

(2 mL) were added. DCM phase was separated and concentrated to obtain diethyl 6-aminohexyl phosphonate as a yellow liquid in 20-30% yield.

FT-IR (ATR): 955, 1019 (P-O-C), 1214 (P=O), 2932 (C-H), 3419 (NH) cm^{-1}.

^{1}H-NMR (400 MHz, $CDCl_3$, δ): 1.27 (6H, $OCH_2\mathit{CH_3}$), 1.51 (8H, $\mathit{CH_2}CH_2$-P), 1.69 (2H, $\mathit{CH_2}$-P), 2.60 (2H, $\mathit{CH_2}NH$), 4.01 (4H, $O\mathit{CH_2}CH_3$) ppm.

2.3.3. Synthesis of Tetraethyl Vinylidene Bisphosphonate

Tetraethyl vinylidene bisphosphonate was prepared from tetraethyl methylene bisphosphonate by the method of Degendardt *et al*. [72]. In the first step, paraformaldehyde (0.26 g, 8.6 mmol), and diethylamine (0.18 mL, 1.6 mmol) were combined in 5 mL of methanol and heated at 37 °C until a clear solution was obtained. Then heat was removed and tetraethylmethyl bisphosphonate (0.43 mL, 1.7 mmol) was added. The mixture was refluxed for 24 h, then an additional 5 mL of methanol was added, and the solution was concentrated under vacuum. Toluene (2.5 mL) was added and the solution was again concentrated. This step was repeated to ensure complete removal of methanol from the product and product was obtained as yellow liquid.

In the second step, the product of the first step, dry toluene (2.5 mL) and pTsOH (2 mg) were refluxed at 115 °C. Methanol was removed from the reaction mixture by a Dean-Stark trap. After 16 hours, the solution was concentrated. The crude product was diluted with 2.5 ml of chloroform and washed with water (2 × 0.4 mL). The chloroform solution was dried over anhydrous Na_2SO_4 and concentrated. Yellow liquid product was obtained in 80% yield.

FT-IR (ATR): 968, 1016 (P-O), 1244 (P=O), 2985 (C-H) cm^{-1}.

^{1}H-NMR (400 MHz, $CDCl_3$, δ): 1.24 (m, 12H, $OCH_2\mathit{CH_3}$), 4.09 (m, 8H, $O\mathit{CH_2}CH_3$), 6.87 (t, 2H, $\mathit{CH_2}$=C) ppm.

2.3.4. Synthesis of Amines Containing Both Phosphonate and Bisphosphonate (A1 and A2)

2.3.4.1.A1. Diethyl (2-aminoethyl)phosphonate (0.298 g, 1.65 mmol) and tetraethyl vinylidene bisphosphonate (0.594 g, 1.98 mmol) were mixed at room temperature for 2 days under inert atmosphere. The reaction mixture was washed with petroleum ether to remove excess tetraethyl vinylidene bisphosphonate and dried under reduced pressure. The product was obtained as yellow liquid with 87% yield.

FT-IR (ATR): 956, 1016 (P-O), 1245 (P=O), 2923 (C-H), 3454 (NH) cm^{-1}.

^{1}H-NMR (400 MHz, $CDCl_3$, δ): 1.35 (m, 18H, OCH_2CH_3), 1.96 (m, 2H, CH_2-P), 2.6 (tt, $^{3}J_{HH}$=6 Hz, J_{HP}=23.6 Hz, 1H, P-CH-P,), 2.88 (m, 2H, CH_2CH_2NH), 3.14 (td, $^{3}J_{HH}$=6 Hz, J_{HP}=16.8 Hz, 2H, $NHCH_2CH$-P), 4.13 (m, 12H, OCH_2CH_3) ppm.

^{13}C NMR (101 MHz, $CDCl_3$, δ): 16.30 (OCH_2-CH_3), 22.94 (CH_2-P), 36.19 (P-CH-P), 46.07 (CH_2-CH_2-NH), 49.13 (NH-CH_2CH-P), 62.54 (O-CH_2-CH_3) ppm.

2.3.4.2.A2. Diethyl (6-aminohexyl)phosphonate (0.24 g, 1 mmol) and tetraethyl ethylidene bisphosphonate (0.3 g, 1 mmol) were mixed and stirred at room temperature for 2 days under inert atmosphere. The reaction mixture was washed with petroleum ether to remove excess tetraethyl vinylidene bisphosphonate and dried under reduced pressure. The product was obtained as yellow liquid with 63 % yield.

FT-IR (ATR): 954, 1016 (P-O), 1239 (P=O), 2932 (C-H), 3476 (NH) cm^{-1}.

^{1}H-NMR (400 MHz, $CDCl_3$, δ): 1.34 (m, 18H, OCH_2CH_3), 1.52 (m, 8H, PCH_2CH_2), 1.70 (m, 2H, CH_2-P), 2.56 (t, $^{3}J_{HH}$=7.2 Hz, 2H, CH_2CH_2NH), 2.66 (dt, $^{3}J_{HH}$=6 Hz, J_{HP}=23,6 Hz, 1H, P-CH-P), 3.12 (td, $^{3}J_{HH}$=6 Hz, J_{HP}=16.8 Hz, 2H, $NHCH_2CH$-P), 4.12 (m, 12H, OCH_2CH_3) ppm.

2.4. Synthesis of Monomers

2.4.1. Synthesis of Acrylamides Containing Both Phosphonate and Bisphosphonate

Acryloyl chloride (0.058 g, 0.65 mmol) in dry DCM (0.5 mL) was added dropwise, under N_2, to an ice cold mixture of A1 or A2 (0.54 mmol), and pyridine or TEA (0.05 g,

0.65 mmol) in dry DCM (1.1 mL). The mixture was stirred at room temperature for 2-5 hours. Then DCM (10 ml) was added to the mixture and it was extracted with distilled water (2 x 8 mL), 2 M HCl (2 x 8 mL), and saturated $NaHCO_3$ (2 x 8 mL). The combined organic layers were dried over anhydrous Na_2SO_4 and DCM was evaporated. The crude product was purified by reversed-phase flash chromatography on C18, eluting with water/methanol (50/50). Monomers were obtained as yellow viscous liquids.

2.4.1.1.AAm-A1. FT-IR (ATR): 957, 1014 (P-O), 1239 (P=O), 1647 (C=C), 1694 (C=O), 2983 (C-H) cm^{-1}.

^{1}H-NMR (400 MHz, $CDCl_3$, δ): 1.27 (m, 18H, OCH_2CH_3), 1.94 (m, 2H, CH_2-P), 3.39 (tt, $^3J_{HH}$=7.6 Hz. J_{HP}=22.8 Hz, 1H, P-C*H*-P), 3.58 (m, 2H, CH_2CH_2NH), 3.75 (m, 2H, $NHCH_2CH$), 4.1 (m, 12H, OCH_2CH_3), 5.64, 6.29 (d, 2H, $CH=CH_2$), 6.51 (m, 1H, $CH=CH_2$) ppm.

2.4.1.2.AAm-A2. FT-IR (ATR): 960, 1016 (P-O), 1222 (P=O), 1643 (C=C), 1704 (C=O), 2935 (C-H) cm^{-1}.

^{1}H-NMR (400 MHz, $CDCl_3$, δ): 1.32 (m, 18H, OCH_2CH_3), 1.50 (m, 8H, PCH_2CH_2), 1.67 (m, 2H, CH_2-P), 3.42 (m, 1H, P-C*H*-P), 3.49 (m, 2H, CH_2CH_2NH), 3.80 (m, 2H, $NHCH_2CH$), 4.13 (m, 12H, OCH_2CH_3), 5.68, 6.33 (d, 2H, $CH=CH_2$), 6.52 (m, 1H, $CH=CH_2$) ppm.

2.4.2. Synthesis of Acrylamides Containing Both Phosphonic and Bisphosphonic Acid

To the ice cold solution of AAm-A1 or AAm-A2 (0.346 mmol) in dry DCM (0.7 mL), TMSBr (0.238 g, 1.56 mmol) was added under nitrogen stream dropwise. The mixture was stirred at 30 °C for 5 hours. DCM and excess TMSBr were evaporated under reduced pressure. MeOH (0.7 ml) was added, and then the mixture was stirred at room temperature for 15 minutes. The solvent was evaporated.

2.4.3. Synthesis of Methacrylates Containing Both Phosphonate and Bisphosphonate

To an ice-cold solution of either A1 or A2 (0.415 mmol) in 1.5 mL of dry chloroform under stream of nitrogen, IEM (0.066 g, 0.430 mmol) was added dropwise. The solution was stirred at room temperature overnight under nitrogen and then extracted with 1 wt% HCl (2 x 6.2 ml) and brine (2 x 6.2 ml). The organic layer was dried over Na_2SO_4, filtered and evaporated under reduced pressure to leave the crude product which was purified by reversed-phase flash chromatography on C18, eluting with water/methanol (50/50). Monomers were obtained as pale yellow viscous liquids.

2.4.3.1.MA-A1. FT-IR (ATR): 953, 1016 (P-O), 1233 (P=O), 1638 (C=C), 1638, 1715 (C=O), 2982 (C-H), 3435 (NH) cm^{-1}.

^{1}H-NMR (400 MHz, $CDCl_3$, δ): 1.30 (m, 18H, OCH_2CH_3), 1.90 (s, 3H, $CH_3C=CH_2$), 2.08 (m, 2H, CH_2-P), 2.85 (tt, $^3J_{HH}$=6 Hz, J_{HP}=23.6 Hz, 1H, P-CH-P), 3.48 (q, $^3J_{HH}$=5.6 Hz, 2H, OCH_2CH_2NH), 3.53 (m, 2H, $NHCH_2CH_2$-P), 3.76 (td, $^3J_{HH}$=6 Hz, J_{HP}=14.4 Hz, 2H, NCH_2CH-P), 4.11 (m, 14H, OCH_2CH_3, $NHCH_2CH_2O$), 5.51, 6.14 (s, 2H, $C=CH_2$) ppm.

^{13}C NMR (101 MHz, $CDCl_3$, δ): 16.27 (OCH_2-CH_3), 18.19 ($CH_3C=CH_2$), 24.19 (CH_2-P), 37.53 (P-CH-P), 39.76 (OCH_2-CH_2-NH), 42.18 (NH-CH_2-CH_2-P), 44.88 (N-CH_2-CH-P), 62.78 (OCH_2CH_3, $NHCH_2$-CH_2-O), 125.57,136.08 ($C=CH_2$), 157.82 (O=C-OCH_2), 167.28 (O=C-NH) ppm.

2.4.3.2.MA-A2. FT-IR (ATR): 958, 1020 (P-O), 1239 (P=O), 1632 (C=C), 1632,1716 (C=O), 2984 (C-H), 3310 (NH) cm^{-1}.

^{1}H-NMR (400 MHz, $CDCl_3$, δ): 1.30 (m, 18H, OCH_2CH_3),), 1.52 (m, 8H, PCH_2CH_2), 1.68 (m, 2H, CH_2-P), 1.91 (s, 3H, $CH_3C=CH_2$), 2.87 (tt, $^3J_{HH}$=5.6 Hz, J_{HP}=23.6 Hz, 1H, P-CH-P), 3.25 (t, $^3J_{HH}$=7.6 Hz, 2H, CH_2CH_2N), 3.49 (q, J=5.6 Hz, 2H, OCH_2CH_2NH), 3.75 (td, $^3J_{HH}$=6 Hz, J_{HP}=14.4 Hz, 2H, CH_2CH-P), 4.11 (m, 14H, OCH_2CH_3, $NHCH_2CH_2O$), 5.55, 6.14 (s, 2H, $C=CH_2$) ppm.

^{13}C NMR (101 MHz, $CDCl_3$, δ): 16.35 (OCH_2-CH_3), 18.27 ($CH_3C=CH_2$), 26.52 (N-$[CH_2]_6$-P), 36.85 (P-CH-P), 40.01 (N-CH_2-CH_2), 44.64 (OCH_2-CH_2-NH), 47.75 (N-CH_2-

CH-P), 62.57 (O*C*$H_2$$CH_3$, NHCH$_2$-*C*H$_2$-O), 125.65, 136.15 (*C*=*C*H$_2$), 157.74 (O=*C*-OCH$_2$), 167.42 (O=*C*-NH) ppm

2.4.4. Synthesis of Methacrylates Containing Both Phosphonic and Bisphosphonic Acid

To the ice cold solution of MA-A1 or MA-A2 (0.346 mmol) in dry DCM (0.7 ml), TMSBr (0.238 g, 1.56 mmol) was added under nitrogen stream dropwise. The mixture was stirred at 30 °C for 5 hours. DCM and excess TMSBr were evaporated under reduced pressure. MeOH (0.7 ml) was added and the mixture was stirred for 15 minutes. The solvent was removed under reduced pressure and the products were obtained as viscous liquid.

2.4.4.1.MA-A1-Ac. FT-IR (ATR): 922, 991(P-O), 1299 (P=O), 1622 (C=C), 1622,1694 (C=O), 2911 (P-O-H), 3309 (NH) cm^{-1}.

^{1}H-NMR (400 MHz, MeOD, δ): 1.92 (s, 3H, C*H*$_3$C=CH$_2$), 2.05 (m, 2H, C*H*$_2$-P), 2.72 (tt, $^3J_{HH}$= 6Hz, J_{HP}=23.2 Hz, 1H, P-C*H*-P), 3.47 (t, $^3J_{HH}$=5.6 Hz, 2H, OCH$_2$C*H*$_2$NH), 3.61 (q, 2H, NC*H*$_2$CH$_2$-P), 3.84 (td, $^3J_{HH}$=6 Hz, J_{HP}=14.4 Hz, 2H, NC*H*$_2$CH-P), 4.21 (t, $^3J_{HH}$=5.6 Hz, 2H, NHCH$_2$C*H*$_2$O), 5.61&6.14 (s, 2H, C=C*H*$_2$) ppm.

^{13}C NMR (101 MHz, D$_2$O, δ): 17.30 (*C*H$_3$C=CH$_2$), 24.97 (*C*H$_2$-P), 36.61 (P-*C*H-P), 39.15 (OCH$_2$-*C*H$_2$-NH), 42.40 (NH-*C*H$_2$-CH$_2$-P), 44.50 (N-*C*H$_2$-CH-P), 126.96,135.65 (*C*=*C*H$_2$), 158.98 (O=*C*-OCH$_2$), 169.62 (O=*C*-NH) ppm.

2.4.4.2.MA-A2-Ac. ^{1}H NMR (400 MHz, MeOD, δ): 1.60 (m, 8H, PCH$_2$-C*H*$_2$), 1.73 (m, 2H, P-C*H*$_2$-CH$_2$), 1.93 (s, 3H, C*H*$_3$C=CH$_2$), 2.67 (tt, $^3J_{HH}$= 5.6 Hz, J_{HP}=23.2 Hz, 1H, P-C*H*-P), 3.31 (m, 2H, N-C*H*$_2$-CH$_2$), 3.46 (t, ^{3}JHH=5.6 Hz, 2H, NC*H*$_2$CH$_2$-P), 3.82 (td, $^3J_{HH}$=6 Hz, J_{HP}=14.4 Hz, 2H, NC*H*$_2$CH-P), 4.20 (t, $^3J_{HH}$=5.6 Hz, 2H, NHCH$_2$C*H*$_2$O), 5.63, 6.13 (s, 2H, C=C*H*$_2$) ppm.

2.5. Etching Performances of Monomers

Enamel and dentin surfaces were prepared by Asst. Prof. Dr. Keziban Olcay. Three human carious-free permanent molar teeth were used for analysis. They were horizontally cut with the aid of a carbon separating disk under water cooling, leaving the dentin open at the coronal portion. In the same way, a horizontal section with a thickness of 4 mm was obtained from the tooth crown with a second incision from the enamel-cement combination. Dentin and enamel surfaces of the tooth sections were grinded under water cooling with 350, 600, 800 and 1200 grit silicon carbide abrasive papers, respectively, to provide smear layer removal and homogenization of surface roughness. Each grinding operation was applied for 1 minute to ensure standardization. The acidic monomer (20 wt%) EtOH / water (1:1 v/v) solution was applied continuously to the enamel and dentin surfaces for 15 seconds. The surfaces were then washed with 2.5 mL of distilled water and then with 1 mL of ethanol and dried with strong air for 5 seconds. Changes on the surface of the samples were examined with SEM.

2.6. HAP Interaction of Monomers

HAP (0.1 g) was dispersed in monomer/EtOH/H_2O (0.5 g, 15:45:40 wt%) mixture by stirring 1 day at room temperature. Monomer coated HAP particles were separated from mixture by centrifugation. The particles were washed with EtOH and H_2O, dried at room temperature. The crystal phases on the monomer-coated HAP particles were identified by a powder XRD operated under 40 kV acceleration, 40 mA current, and scanning rate of 2° min^{-1} for $2\theta/\theta$ scan [73].

2.6.1. FTIR

Monomer treated HAP particles, prepared as mentioned above, and their solution phase were analyzed by FTIR.

2.6.2. XRD

Crystal phase of treated HAP particles was examined by XRD.

2.6.3. XPS

Crystal phase of treated HAP particles was examined by XPS.

2.7. Photopolymerization

Photopolymerization kinetics of the monomers were analyzed by two different methods: photo-DSC and real-time FTIR spectroscopy.

Photo-DSC: 3.0 – 4.0 mg sample was placed on an aluminum DSC plate. Photoinitiator (2 mol% of sample) was added. Before (5 min) and during polymerization (5 min), nitrogen gas was passed. Samples were exposed to light for 5 minutes at 37 °C (mercury arc lamp, light intensity 20 mW / cm^2), and heat evolved during polymerization was recorded under isothermal conditions. Polymerization rate and yield were determined. Theoretical polymerization heat (ΔH_p) was taken as 20.6 and 13.0 kcal/mol for acrylamide and methacrylate, respectively, and polymerization rate was calculated by the following formula.

$$Rate = \frac{(Q/s)M}{n\,\Delta H_p\,m} \qquad (2.1)$$

In this formula, Q/s is heat evolved during polymerization, M is the molecular weight of the monomer, n is the number of double bonds, and m is mass of monomer.

Real-time FTIR spectroscopy: Monomer-photoinitiator (98:2 mol%) mixtures were photopolymerized by real-time FTIR spectroscopy (Nicholet 6700). Mercury arc lamp (Omnicure s1000 – 100 W) was used as the light source. Change in double bond of monomer (approximately 1643 cm^{-1}) was continuously monitored by taking carbonyl (1700 cm^{-1}) as reference. Polymerization yield (conversion) was calculated by the following formula.

$$Conversion\ \% = \left(1 - \frac{Abs_{1643}^{sample}/Abs_{1700}^{sample}}{Abs_{1643}^{monomer}/Abs_{1700}^{monomer}}\right) \times 100 \quad (2.2)$$

2.8. *In vitro* Cytotoxicity Assay

Cytotoxicity test was conducted for MA-A2 and MA-A2-Ac on mouse fibroblast cells (NIH 3T3). Cells were cultured in RPMI 1640 medium, supplemented with 10 % FBS and 1 % penicillin/streptomycin antibiotic solution, according to ATCC recommendations. Cells were grown in a 5 % CO_2-humidified incubator at 37 °C. Trypsin–EDTA was used for detachment of cells. To evaluate the cytotoxicity of the synthesized monomers on NIH 3T3cells, MTT cell viability assay was performed. All of the cells were seeded at a density of 1 x 10^4 cells/well into 96-well plates. The next day, the medium was removed and different concentrations of the monomers (10-200 μM) were added with fresh culture medium. After 24 h incubation, the medium in each well was replaced with 150 μL culture medium and 50 μL of MTT solution (5 mg/mL in PBS) which forms purple formazan as a consequence of mitochondrial activity of viable cells. The cells were then further incubated for 4 h and then EtOH:DMSO (1:1 v/v) solution was added to wells and subjected to a gentle shaking for 15 min to dissolve formazan crystals. Absorbance intensity at 600 nm was measured with a reference wavelength of 630 nm using a ELx800™ Absorbance Microplate Reader (BioTek Instruments, Inc., Vermont, United States). Cells without any treatment were used as controls under the assumption of 100 % viability. Relative cell viability was calculated according to the formula:

$$Cell\ viability\ (\%) = \left[\frac{sample\ absorbance}{control\ absorbance}\right] x\ 100 \quad (n = 5) \quad (2.3)$$

Statistical analysis of the polymers was performed using the non-parametric Kruskal–Wallis test with Dunn's multiple comparison post-test or Mann-Whitney test of GraphPad Prism 6 software package (GraphPad Software, Inc., USA). Data were reported

as mean values ± standard deviation (S.D.). All tests were two-tailed and the differences between measurements were considered statistically significant if $p < 0.05$.

2.9. Thermal Copolymerization

2.9.1. Synthesis of AAm-A2-*co*-PEGMA copolymer

The copolymerization of AAm-A2 and PEGMA (50:50 and 20:80 mol% feed ratios) was carried out in MeOH under nitrogen at 60 °C with AIBN as initiator.

2.9.1.1. AAm-A2-*co*-PEGMA (50:50 mol%). AAm-A2 (50 mg, 0.085 mmol), PEGMA (80 mg, 0.085 mmol) and AIBN (1.5 mg) mixture was dissolved in 0.2 mL MeOH, kept under nitrogen stream for 30 min, and stirred at 60°C for 2 hours. The copolymer was purified by dissolving in DCM and precipitating in diethyl ether, and then was dried under vacuum. Yield: 44%

2.9.1.2. AAm-A2-*co*-PEGMA (20:80 mol%). AAm-A2 (27.9 mg, 0.047 mmol), PEGMA (178 mg, 0.188 mmol) and AIBN (4 mg) mixture was dissolved in 0.2 mL MeOH, kept under nitrogen stream for 30 min, and stirred at 60 °C for 2 hours. The copolymer was purified by dissolving in DCM and precipitating in diethyl ether, and then was dried under vacuum.

2.9.2. Deprotection of AAm-A2-*co*-PEGMA copolymer

To the solution of AAm-A2-*co*-PEGMA copolymer (20:80 mol% feed ratio, 90 mg, 0.1 mmol) in dry DCM (0.2 mL), TMSBr (69 mg, 0.45 mmol) was added slowly at 0 °C under nitrogen. The mixture was stirred for 5 hours at 30 °C. DCM and TMSBr were removed under reduced pressure, MeOH (0.2 mL) was added and stirred for 15 min. After evaporation of MeOH, the pure product was obtained as white powder in 82% yield.

3. RESULTS

3.1. Synthesis and Characterization of Monomers

Two novel amines, A1 and A2, were synthesized and used as starting materials for dental monomers. The starting compounds of these amines, tetraethyl vinylidenebisphosphonate, diethyl (2-aminoethyl)phosphonate and diethyl (6-aminohexyl)phosphonate, were synthesized acccording to the literature procedures [68-72]. Tetraethyl vinylidenebisphosphonate was synthesized in two steps: (i) reaction of tetraethyl methylene bisphosphonate with paraformaldehyde in the presence of a catalyst (diethyl amine) to give an intermediate [$CH_3OCH_2CH(PO_3Et_2)_2$], (ii) elimination reaction of the intermediate catalyzed by pTsOH [72] (Figure 3.1). Diethyl (2-aminoethyl)phosphonate was synthesized from the reaction of diethyl vinylphosphonate and ammonium hydroxide in 30% yield [68]. Diethyl (6-aminohexyl)phosphonate synthesis involved three steps: (i) synthesis of 6-bromohexylphthalimide from the reaction of potassium phthalimide and 1,6-dibromohexane, (ii) conversion of 6-bromohexylphthalimide to 6-phthalimidehexylphosphonate by the reaction of triethyl phosphite, (iii) reaction of 6-phthalimidehexylphosphonate with hydrazine monohydrate [69-71].

A1 and A2 were synthesized from the Michael addition reaction of diethyl (2-aminoethyl)phosphonate or diethyl (6-aminohexyl)phosphonate and tetraethyl vinylidenebisphosphonate (Figure 3.2). Different tetraethyl ethylidenebisphosphonate/amine ratios were tried and best results were obtained when this ratio was 1 or greater than 1 (1.2, 1.3). After removal of excess tetraethyl vinylidenebisphosphonate by washing with petroleum ether, A1 and A2 were obtained as yellow viscous liquids in 87% and 63% yield, respectively. These amines are soluble in water, methanol, dichloromethane and THF, but insoluble in nonpolar solvents such as petroleum ether and hexane (Table 1). The structures of the amines were confirmed by ^1H and FTIR spectroscopies (Figure 3.3). The ^1H NMR spectrum of A1 showed peaks characteristic of methyl protons at 1.35 ppm; methylene protons adjacent to phosphonate at 1.96 ppm; bisphosphonate methine proton at 2.6 ppm (triplet of triplet); methylene protons

adjacent to nitrogen at 2.88 (multiplet) and 3.14 (doublet of triplet) ppm; and two different methylene protons adjacent to oxygen at around 4.13 ppm. In the ^{1}H NMR spectrum of A2, additional peaks due to methylene protons were observed between 1.3 and 1.6 ppm (Figure 3.4). The FTIR spectra of each amine showed stretching peaks of NH, P=O and P-O at 3450, 1239 and 950, 1016 cm^{-1}, respectively (Figure 3.4).

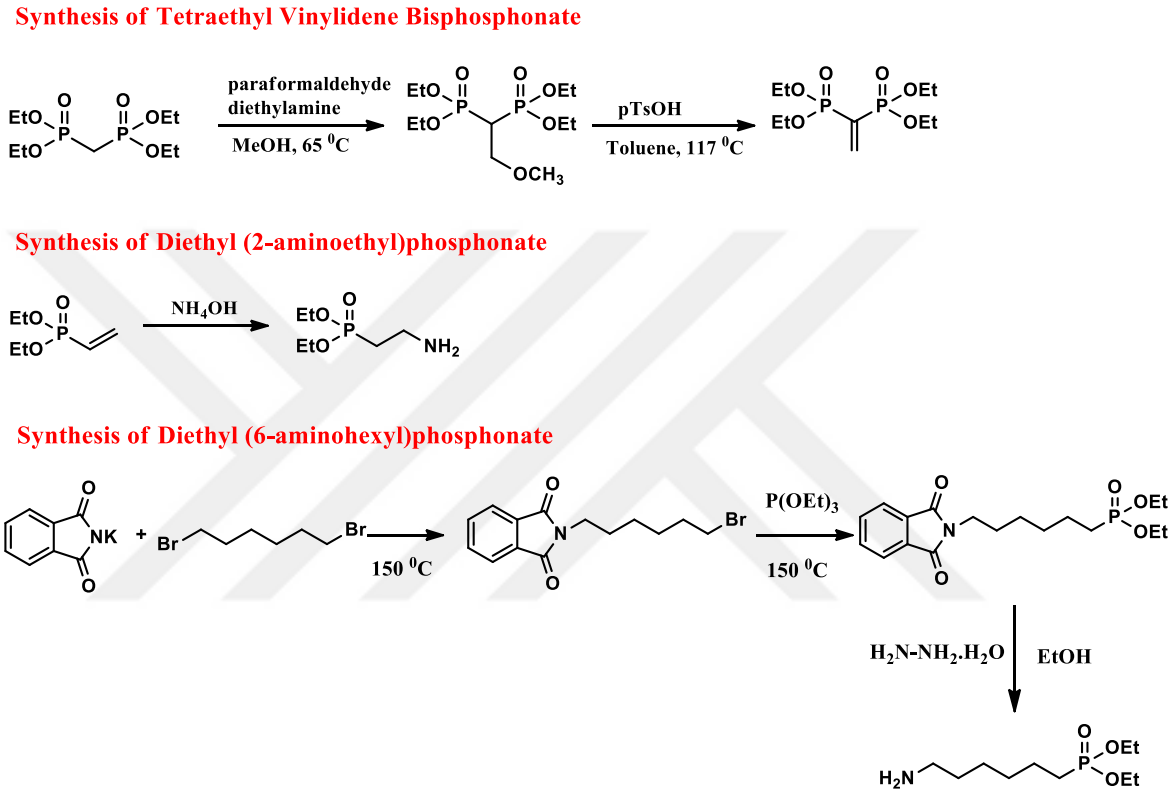

Figure 3.1. Synthesis of starting materials of A1 and A2

A1 and A2 were reacted with acryloyl chloride in the presence of TEA or pyridine catalyst to form both phosphonate and bisphosphonate-containing acrylamides (AAm-A1 and AAm-A2) as yellow viscous liquids in 50-58% yield (Figure 3.2). Monomers were soluble in H_2O, MeOH, diethyl ether and THF but insoluble in petroleum ether (Table 4.1). In the ^{1}H NMR spectrum of AAm-A1 methyl, methylene, and methine protons adjacent to phosporus, methylene protons next to nitrogen were observed at 1.27, 1.94, 3.39, 3.58 and 3.75 ppm respectively. The methylene protons next to oxygen and double bond protons appeared at 4.1, 5.64, 6.29 and 6.51 ppm (Figure 3.5). The structure of AAm-A2 was also

confirmed by ^{1}H NMR and FTIR spectrum (Figure 3.6). In the FTIR spectra, C=O, C=C, P=O and P-O peaks appeared at 1704, 1643, 1222, 1016 and 960 cm^{-1} respectively.

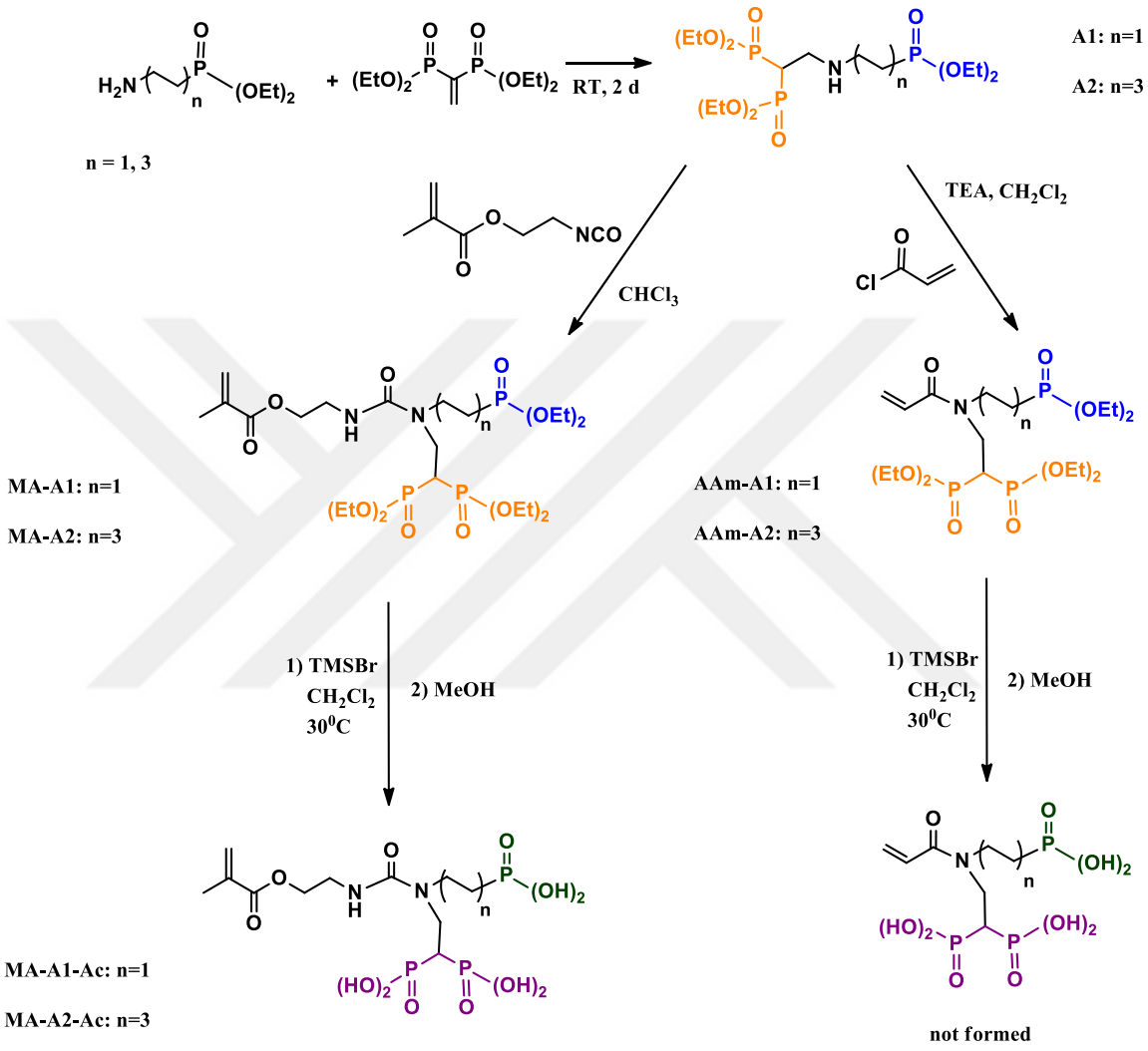

Figure 3.2. Synthesis of A1, A2, AAm-A1, AAm-A2, MA-A1, MA-A2, MA-A1-Ac, and MA-A2-Ac

The phosphonate and bisphosphonate groups of AAm-A1 and AAm-A2 were aimed to be converted into phosphonic and bisphosphonic acid by dealkylation reaction with TMSBr. However, as a result of this reaction, double bond of acrylamide group was almost disappeared. Two different pathways were considered to eliminate the disappearance of the double bond. First pathway was to synthesize methacrylamide

monomers instead of acrylamide ones. Because of the steric hindrance, it was considered that methacrylamide monomers would not polymerize and would have low copolymerization reactivity with dental monomers, so this pathways wasn't followed. Second way was to react A1 and A2 with 2-isocyanatoethyl methacrylate and synthesize

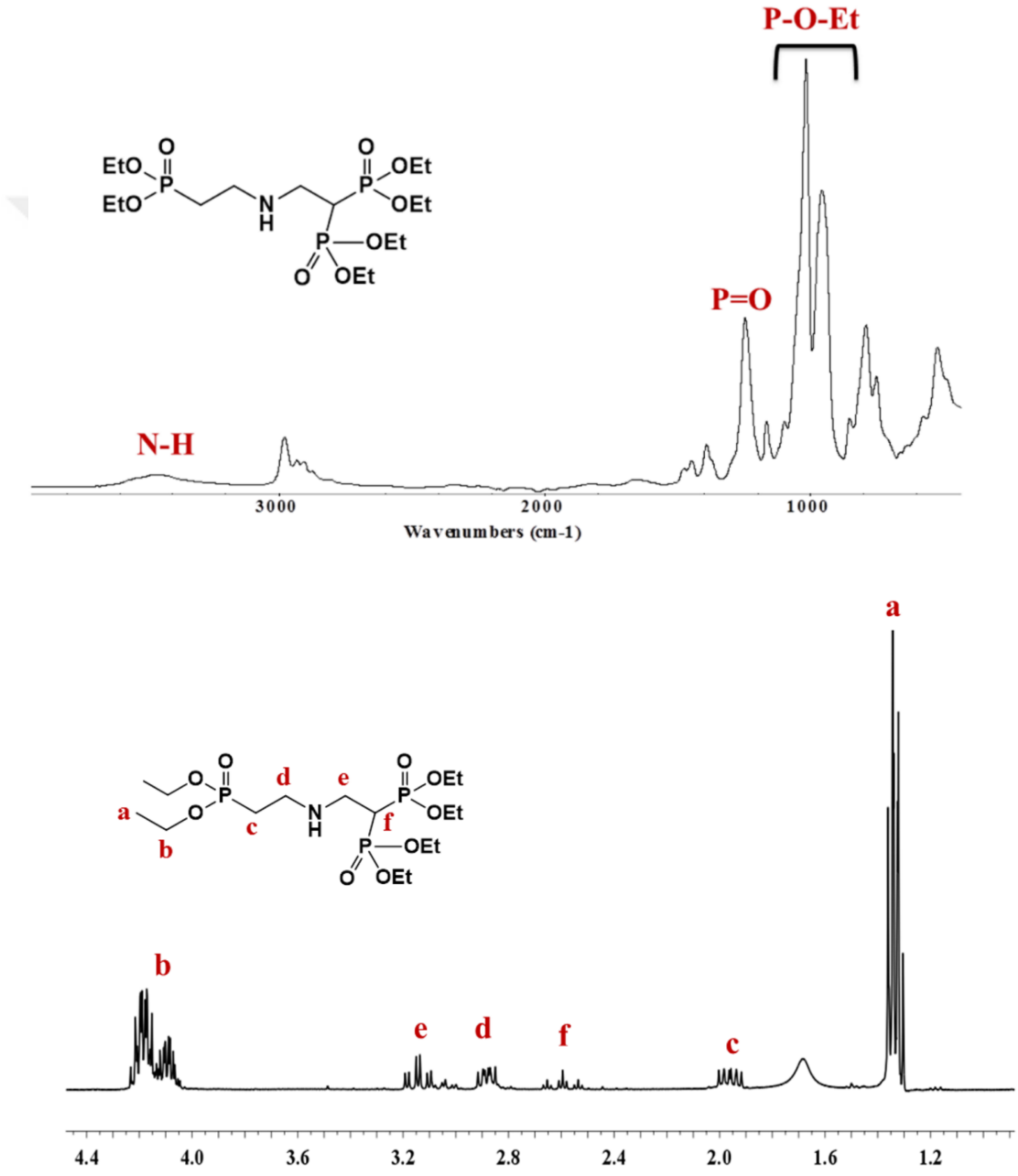

Figure 3.3. FTIR and ^{1}H NMR spectra of A1

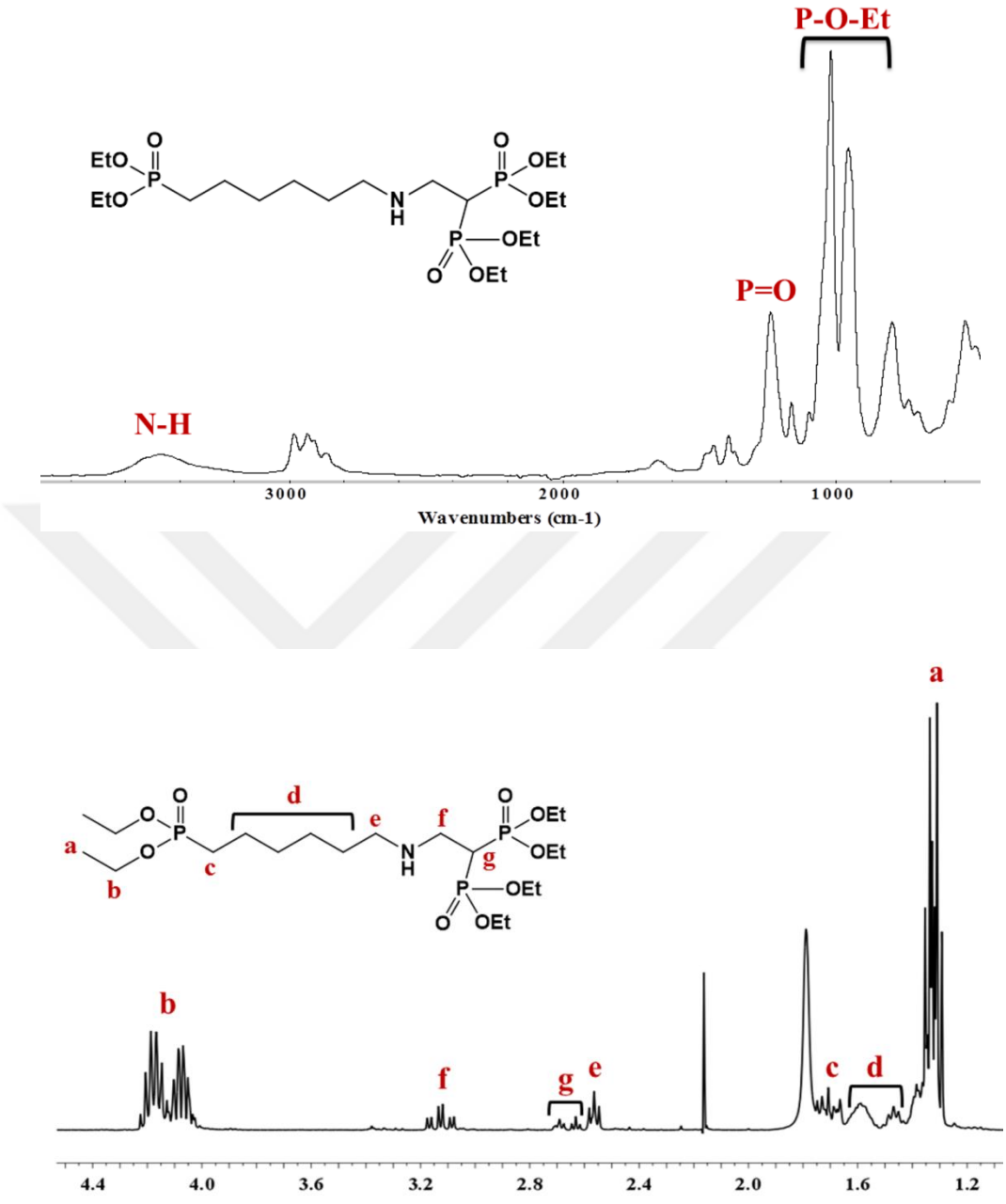

Figure 3.4. FTIR and ^{1}H NMR spectra of A2

methacrylate monomers with high polymerization reactivity (Figure 3.2). Two novel methacrylate monomers were synthesized with this method, and purified with flash chromatography. These monomenrs (MA-A1 and MA-A2), were obtained as yellow viscous liquids in 60-67% yield. Structures of these monomers were verified with ^{1}H, ^{13}C NMR and FTIR spectroscopy (Figure 3.7-3.9). In the ^{1}H NMR spectrum of MA-A1, peaks at 2.08 (multiplet), 2.85 (triplet of triplet) and 3.76 (doublet of triplet) ppm are due to

methylene protons adjacent to phosphorus, methine and methylene protons next to nitrogen respectively. Urea hydrogen protons were observed around 6.5 ppm. In the ^{13}C spectrum of this monomer, methylene carbons adjacent to phosphorus and oxygen were observed as doublet, while the methine carbon next to phosphorus was observed as a triplet. In the FTIR spectrum, NH (3435 cm^{-1}), two different C=O (1638 and 1715 cm^{-1}), P=O (1233 cm^{-1}), and P-O (953 and 1016 cm^{-1}) stretchings can be seen. Similar peaks were observed in ^{1}H, ^{13}C and FTIR spectra of MA-A2 (Figure 3.8&3.9).

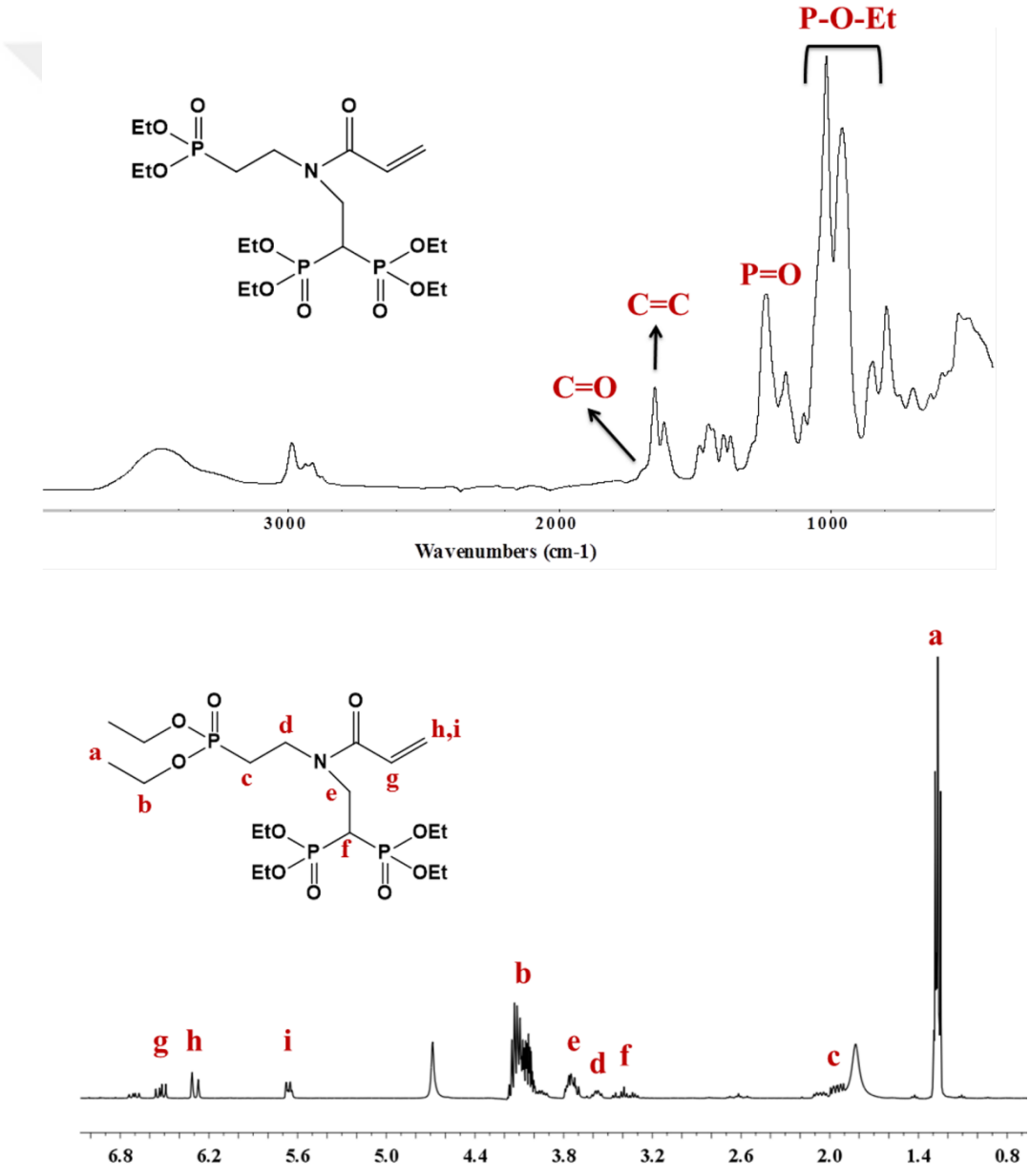

Figure 3.5. FTIR and ^{1}H NMR spectra of AAm-A1

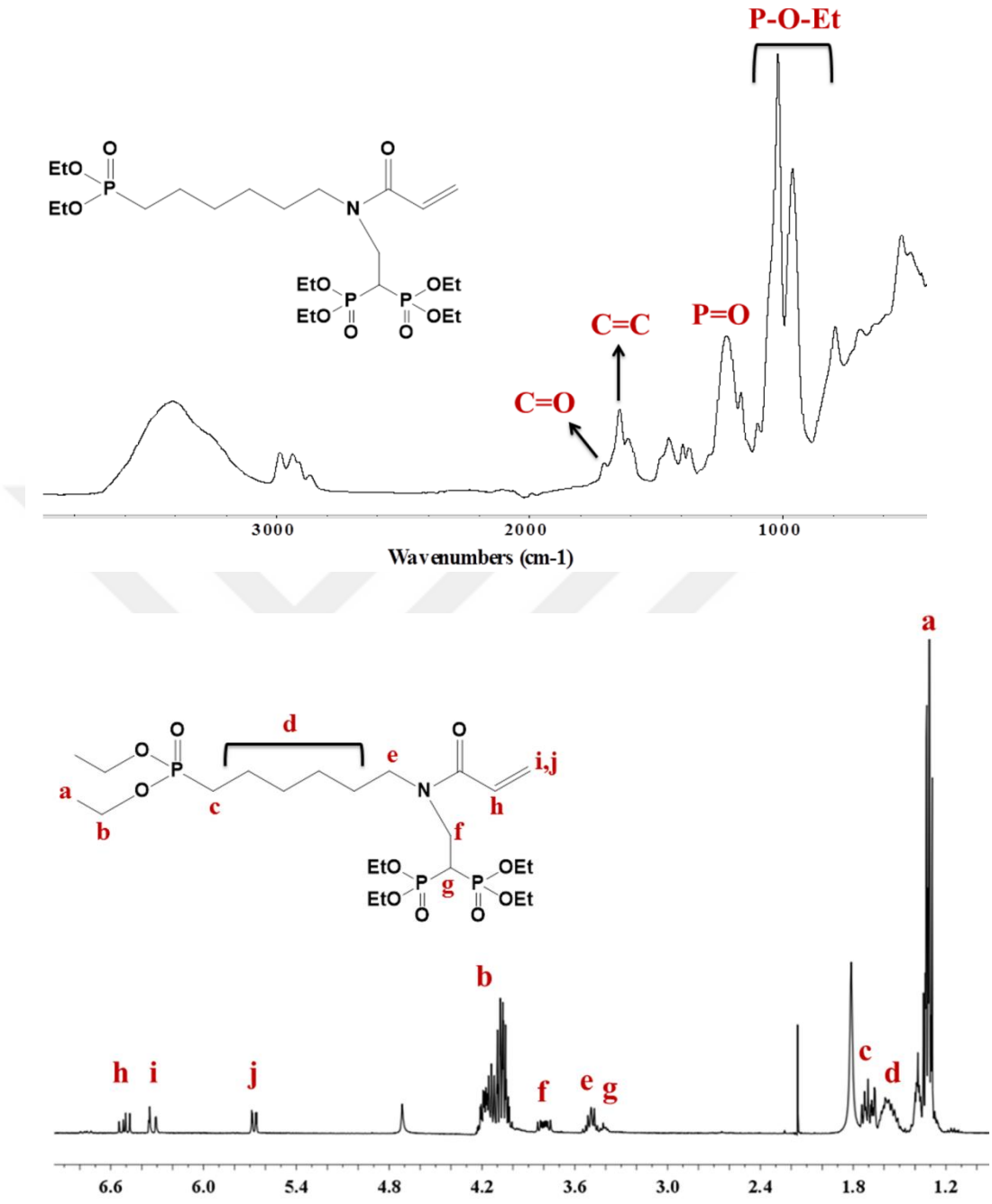

Figure 3.6. FTIR and ^{1}H NMR spectra of AAm-A2

Methacrylate monomers containing phosphonic and bisphosphonic acid groups (MA-A1-Ac and MA-A2-Ac) were synthesized by dealkylation of phosphonate and bisphosphonate groups of MA-A1 and MA-A2 with TMSBr (Figure 3.2). The structures of the monomers were confirmed with ^{1}H and FTIR spectra (Figure 3.10&3.11). The ethyl protons which were present at 1.3 and 4.1 ppm in the ^{1}H NMR spectrum of MA-A1 were

disappeared in the ^{1}H NMR spectrum MA-A1-Ac (Figure 3.10). In the FTIR spectrum of MA-A1-Ac, NH and OH (2000-3000 cm^{-1}), two different C=O (1622 and1694 cm^{-1}), P=O (1299 cm^{-1}), and P-O (922 and 991 cm^{-1}) peaks were observed.

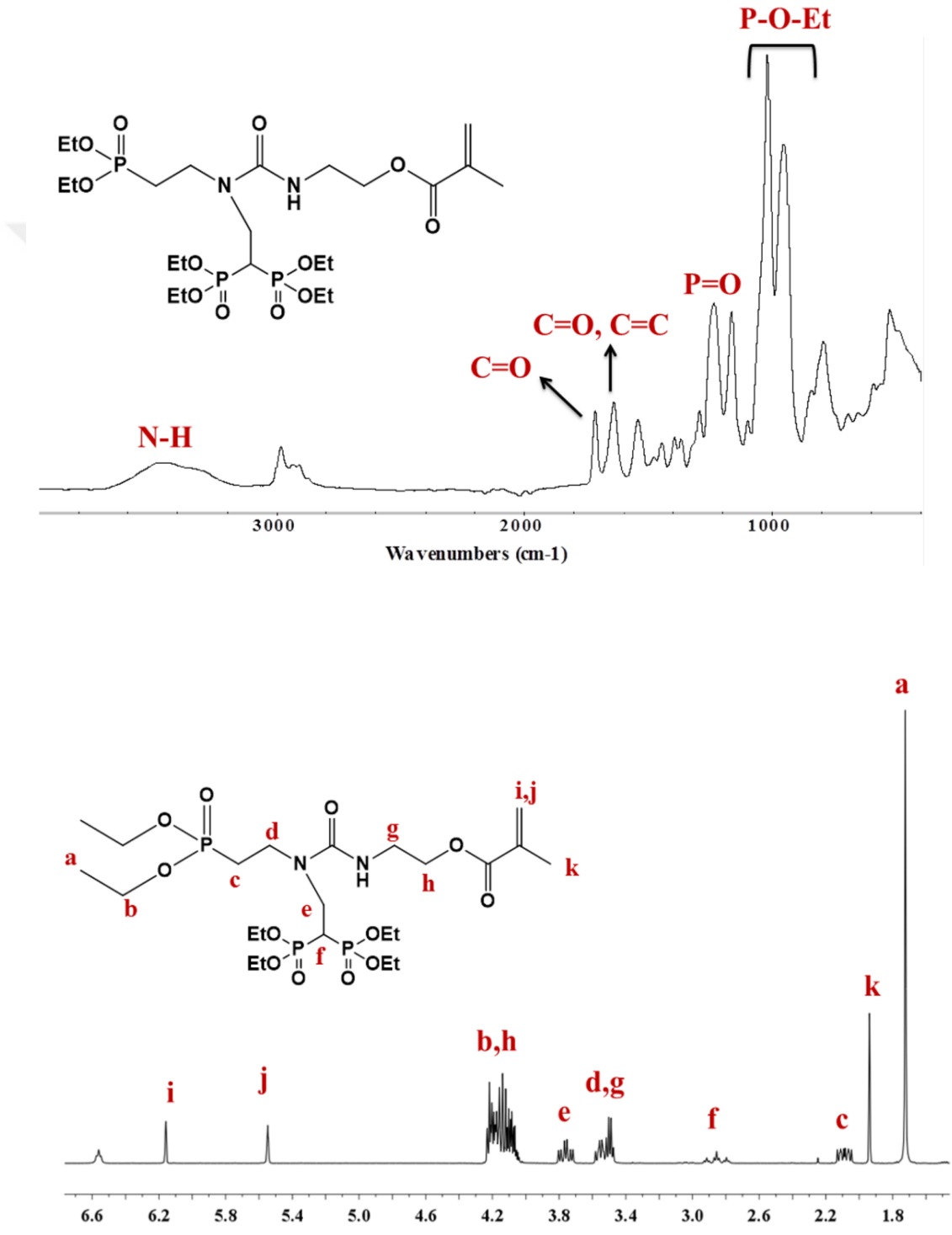

Figure 3.7. FTIR and ^{1}H NMR spectra of MA-A1

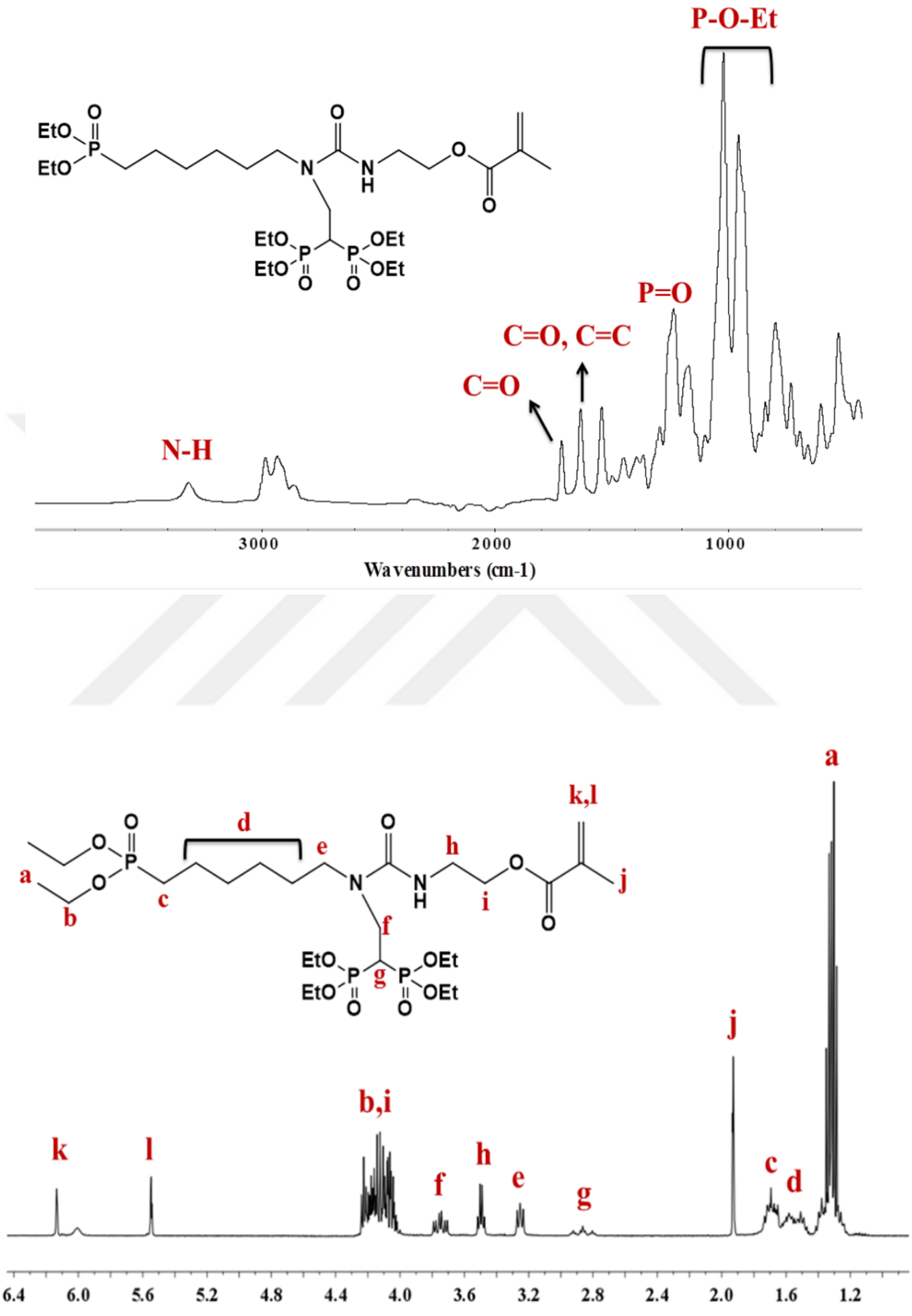

Figure 3.8. FTIR and ^{1}H NMR spectra of MA-A2

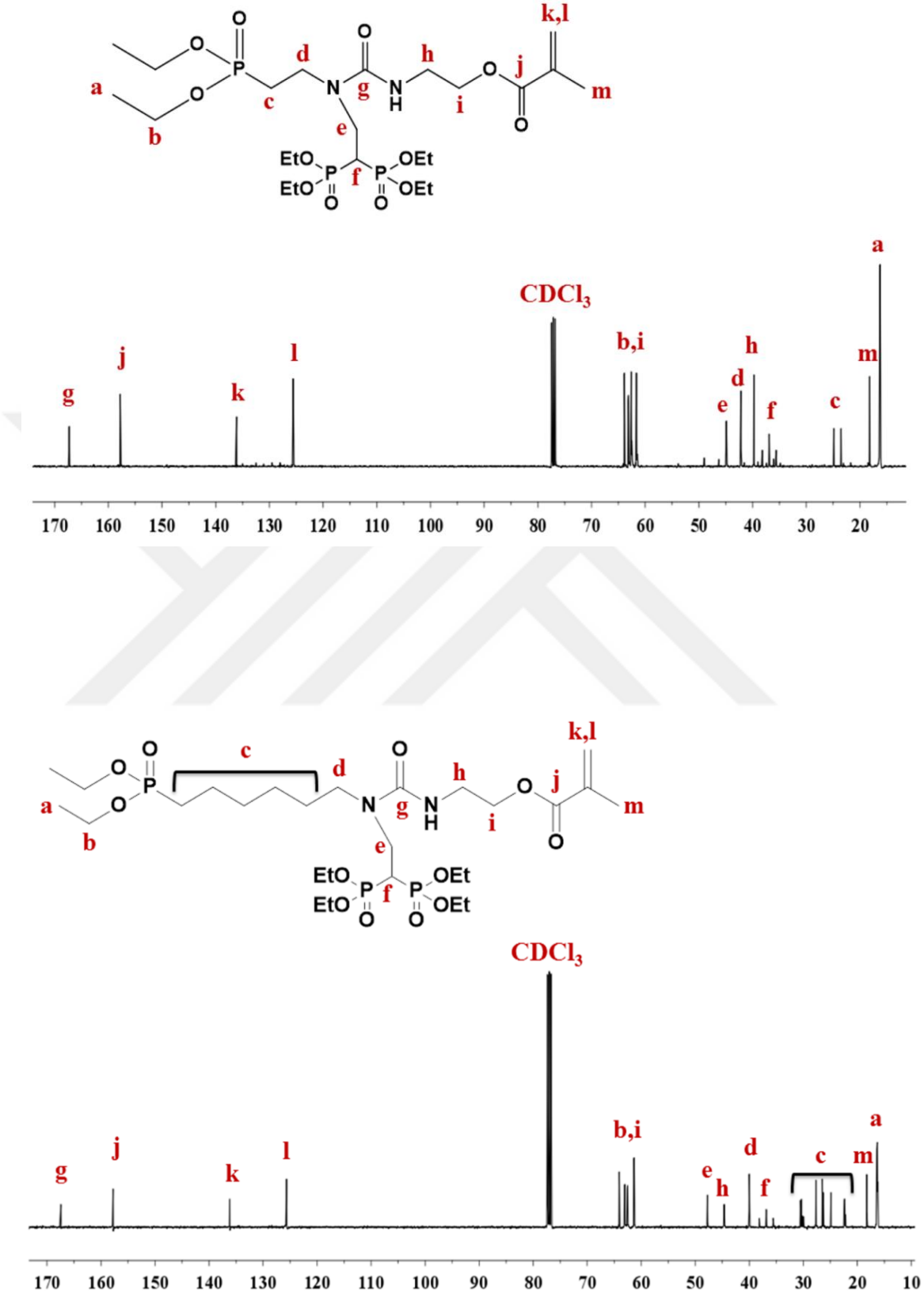

Figure 3.9. ^{13}C NMR spectra of MA-A1 and MA-A2

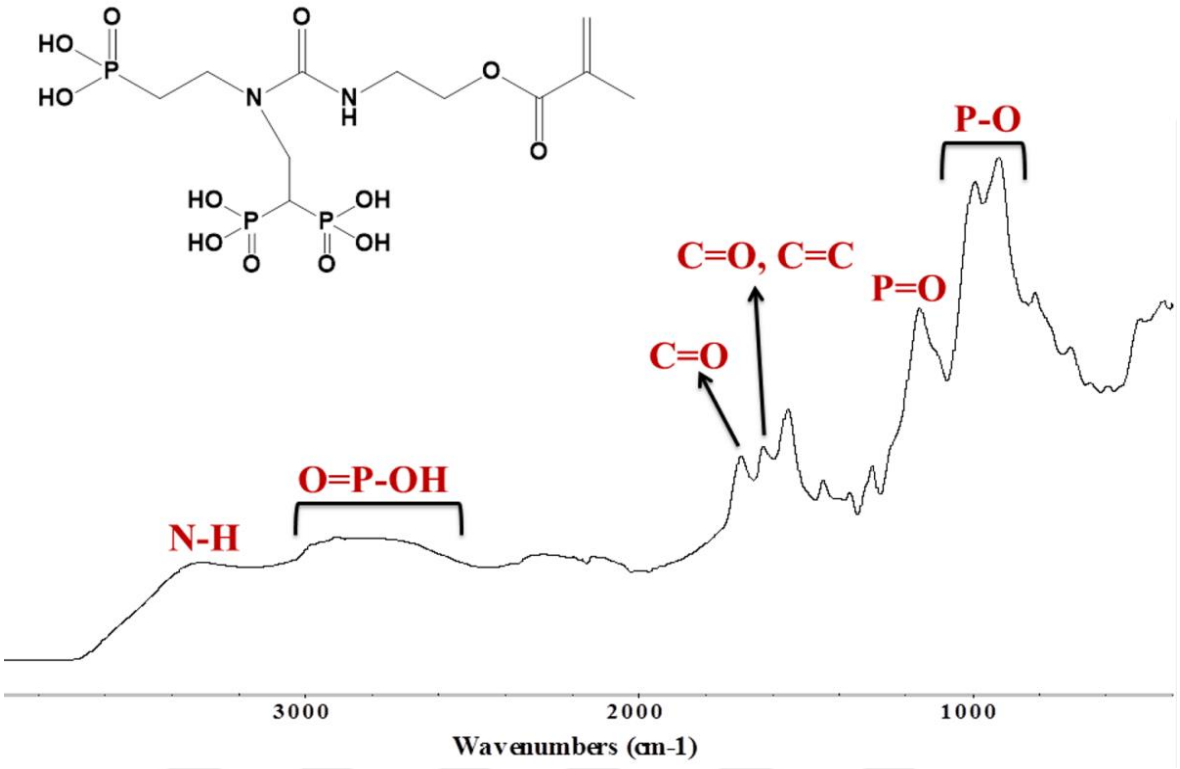

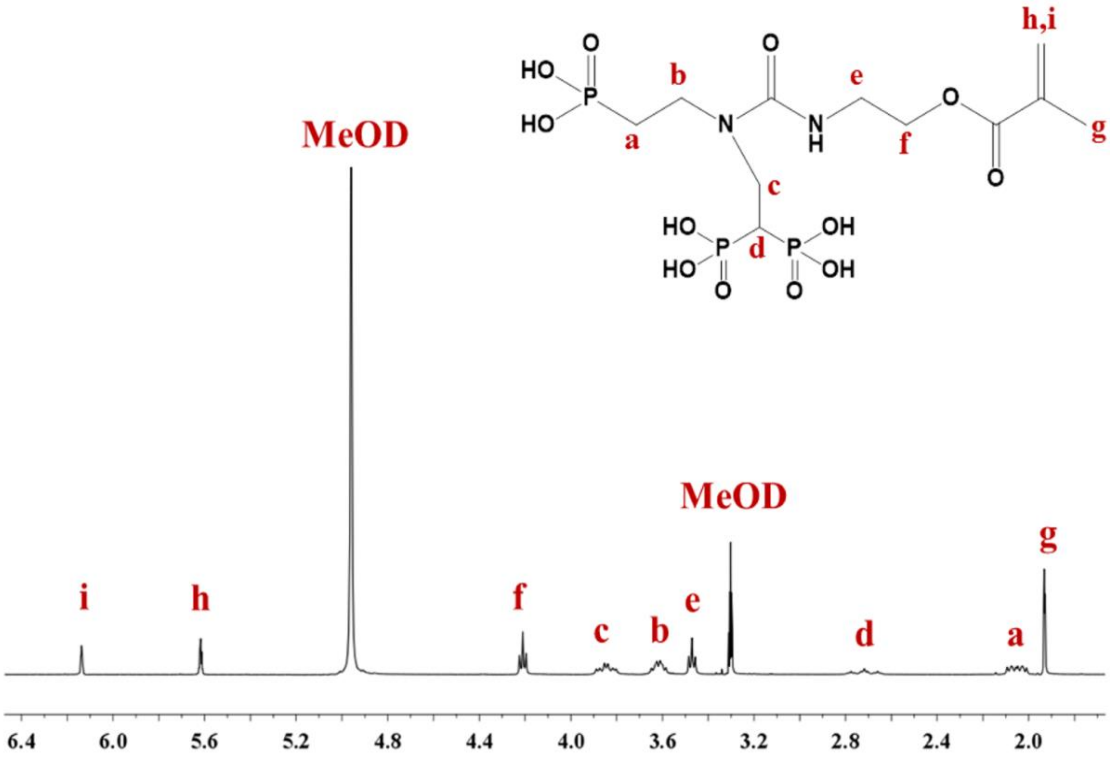

Figure 3.10. FTIR and ^{1}H NMR spectra of MA-A1-Ac

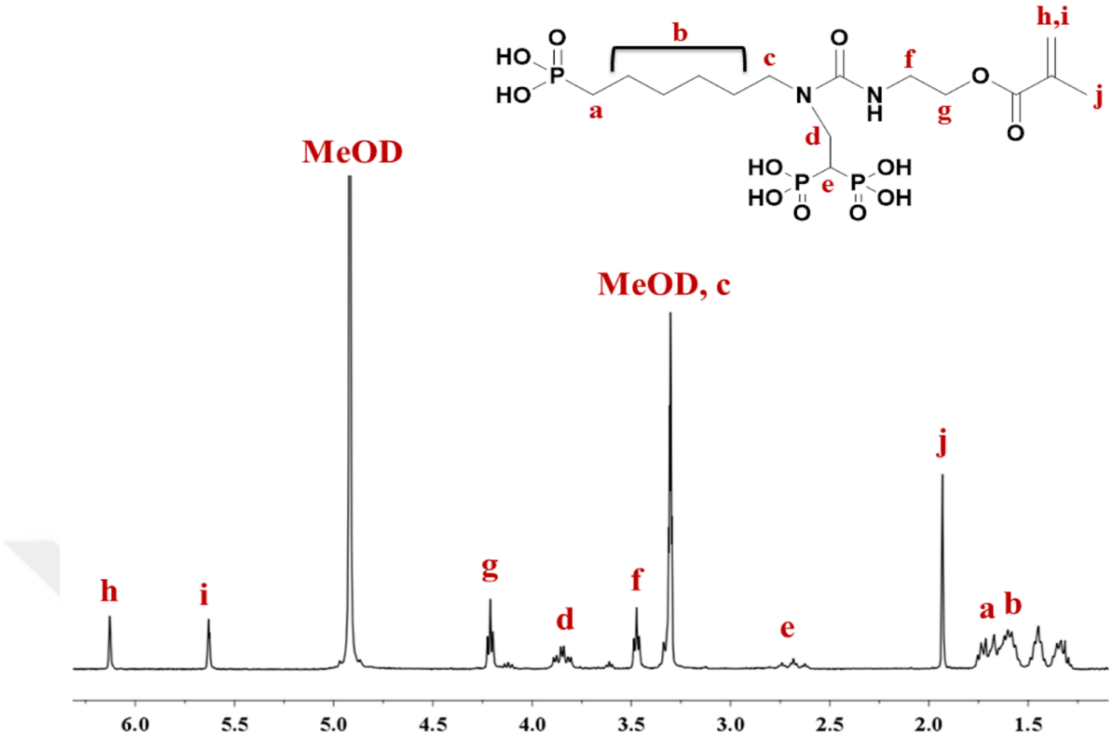

Figure 3.11. ^{1}H NMR spectrum of MA-A2-Ac

3.2. Acidity and HAP Interactions of Monomers

pH values of 1 w% aqueous solutions of MA-A1-Ac and MA-A2-Ac were found to be 1.65 and 1.66 respectively. These values were in the range of mild self-etching monomers (pH ~ 2). The etching performance of MA-A2-Ac was determined by applying EtOH/water solution of the acidic monomer (20 w%) on tooth surface for 15 seconds. After washing with distilled water, ethanol and drying, SEM images of the tooth surface were investigated (Figure 3.12). They showed hydroxyapatite crystals on enamel, partial disappearance of smear layer and demineralization on dentin. These results show that MA-A2-Ac can be used as an etching primer.

Interaction between HAP and acidic monomers was investigated with FTIR, XPS and XRD analysis. Monomer treated HAP particles were prepared as described in the literature [73]. In the FTIR spectrum of EtOH/H_2O phase of MA-A1-Ac treated HAP particles, there were changes in P=O and P-O peaks of the monomer (Figure 3.13). In MA-

A1-Ac, symmetric and asymmetric P-O peaks at 990 and 922 cm^{-1} were shifted and decreased in intensity. Also new peak formed at 1105 cm^{-1}. These changes indicate that MA-A1-Ac demineralized HAP. In the FTIR spectrum of HAP particles treated with MA-A2-Ac, C=O peak was observed which indicated monomers can bind to HAP and form stable salt with it (Figure 3.14).

Interaction between HAP and MA-A2-Ac was also investigated with XPS spectroscopy and compared with that of the commercial monomer, MDP. In the narrow scan spectrum of monomer treated HAP particles, intensity of C1s peak increased compared to HAP (Figure 3.15). This peak was the combination of three peaks: C-C, C-H, C=C binding peak (284.6 eV), C-O binding peak (286 eV), and COO (ester) peak (288 eV). Increase in C1s peak shows that MA-A2-Ac interacted with HAP like MDP.

MA-A2-Ac treated HAP particles were analyzed by XRD (Figure 3.16). The peak at ~5 θ is due to the monomer-Ca salt ($CaMHP_2$) adsorbed onto HAP surface. The salt formed by Ca ions decalcified from HAP.

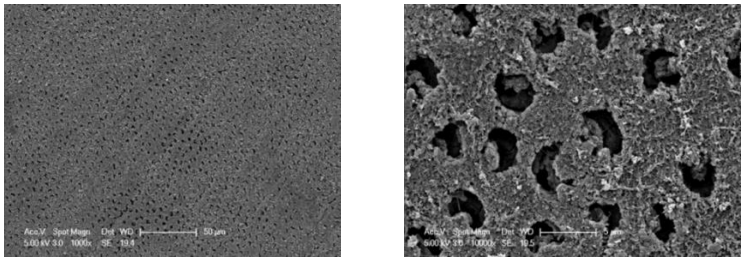

Figure 3.12. SEM image of dentin etched with 20 w% MA-A2-Ac containinng EtOH/H_2O (v/v) solution, 1000 x (left) vs 10000 x (right)

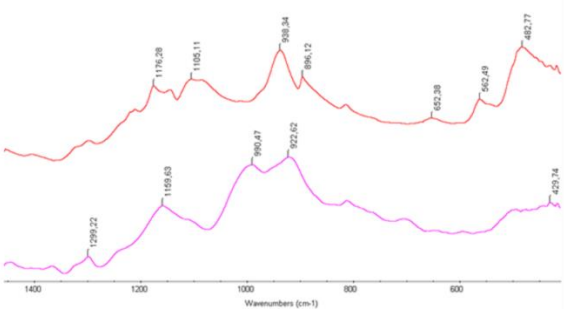

Figure 3.13. FTIR spectra of EtOH/H_2O phase of MA-A1-Ac treated HAP (top spectra) and MA-A1-Ac (bottom spectra)

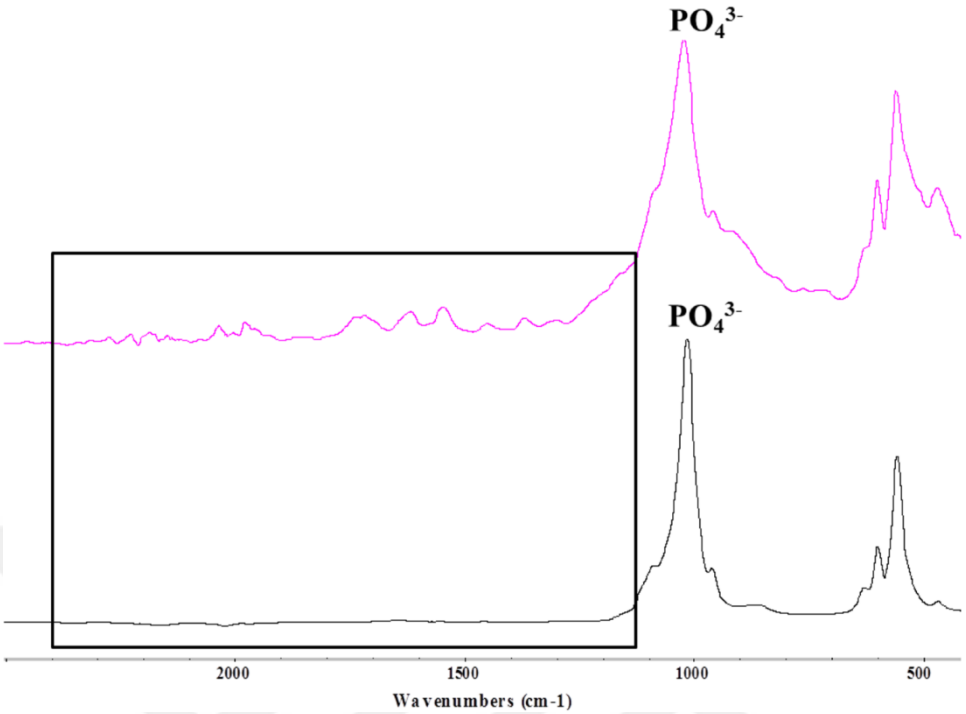

Figure 3.14. FTIR spectra of HAP (bottom spectra) and MA-A2-Ac treated HAP (top spectra)

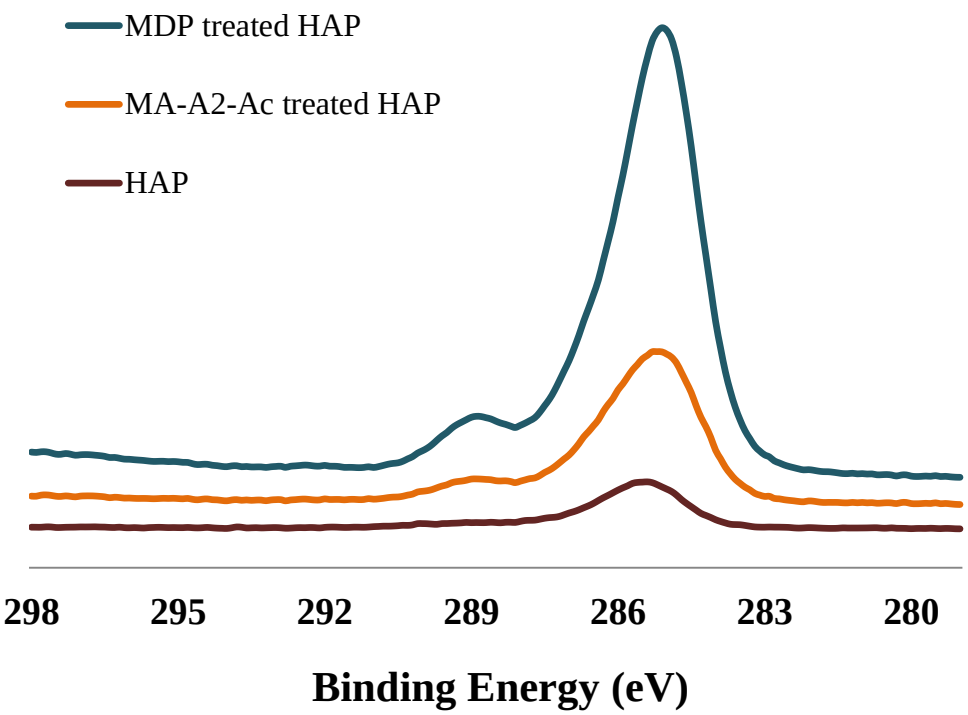

Figure 3.15. XPS spectrum of HAP (bottom spectra), HAP treated with MA-A2-Ac (middle spectra), and MDP treated HAP (top spectra)

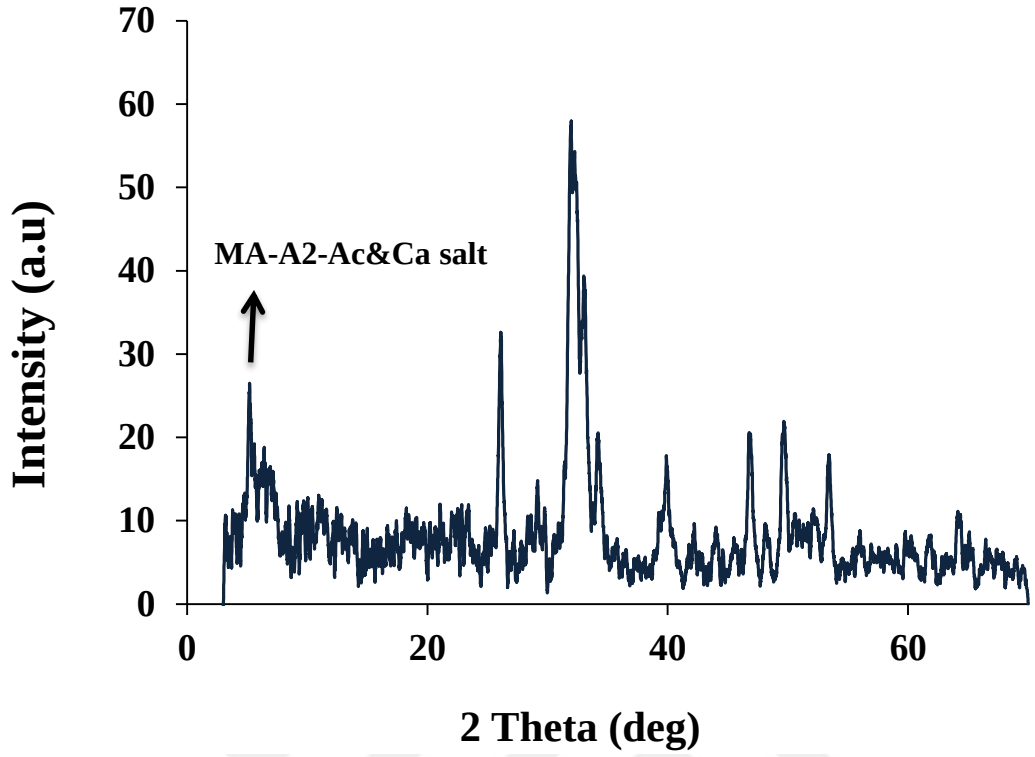

Figure 3.16. XRD spectra of MA-A2-Ac treated HAP

3.3. Photopolymerization

The photopolymerization reactivities of AAm-A1 and AAm-2 were investigated by real time-FTIR using DMPA (2 mol%) as photoinitiator. First, the monomers were mixed with different amounts of HEMA (80 and 90 mol%), most commonly used monomer in dental composites and adhesives, and the mixtures were photopolymerized at two different temperatures (25 and 40 °C) (Figure 3.17). It was observed that addition of increasing fraction of AAm-A1 or AAm-A2 to HEMA resulted in gradual decreases both in rate and conversion. This decrease can be explained by the steric hindrance due to the bulky phosphonate and bisphosphonate groups close to the double bond. Also, polar nature of the synthesized monomers causes high inter- and intramolecular forces and decreases the flexibility of the system, and causes an increase in T_g and reduction in conversion. AAm-A1 and AAm-A2 were also added to Bis-GMA:TEGDMA mixture in different amounts (5, 10 and 20 mol%) and the mixtures were photopolymerized at 25 and 40 °C respectively. The results showed that the synthesized monomers led to lower rates and conversions, similar to the HEMA mixtures (Figure 3.18).

Polymerization behaviours of MA-A1 and MA-A2 with dental monomers were investigated with photo-DSC at 37 °C by using DMPA (2 mol%) as photoinitiator. Bis-GMA is highly viscous compound due to hydrogen bonding. Its high viscosity leads to low homopolymerization conversion. Therefore, Bis-GMA is mixed with TEGDMA, a reactive diluent, to increase its polymerization yield. Formulations consisting of Bis-GMA:TEGDMA:MA-A1 or MA-A2 (50:40:10, 50:30:20 mol%) were prepared and photopolymerized. Figure 3.19-3.20 show photopolymerization results, maximum rate of polymerization (R_{pmax}), and conversion. It was observed that replacement of 10 or 20 mol% of TEGDMA with MA-A1 and MA-A2 increased both the rate and conversion significantly. This increase can rise from lower viscosity, higher reactivity and/or lower double bond count of synthesized monomers than that of TEGDMA. They have the capability of hydrogen bonding due to the urea linkage in their structures, which is an important factor of rate enhancement. In these monomers, phosphonate and bisphosphonate groups are not close to double bond which leads to higher reactivity and conversion besides hydrogen bonding. It is known that increased functionality of a monomer decreases its conversion. Thus, replacement of TEGDMA with the synthesized monofunctional monomers increases the conversions, as expected. These findings shows that MA-A1 and MA-A2 can be used as reactive diluent in dental composites.

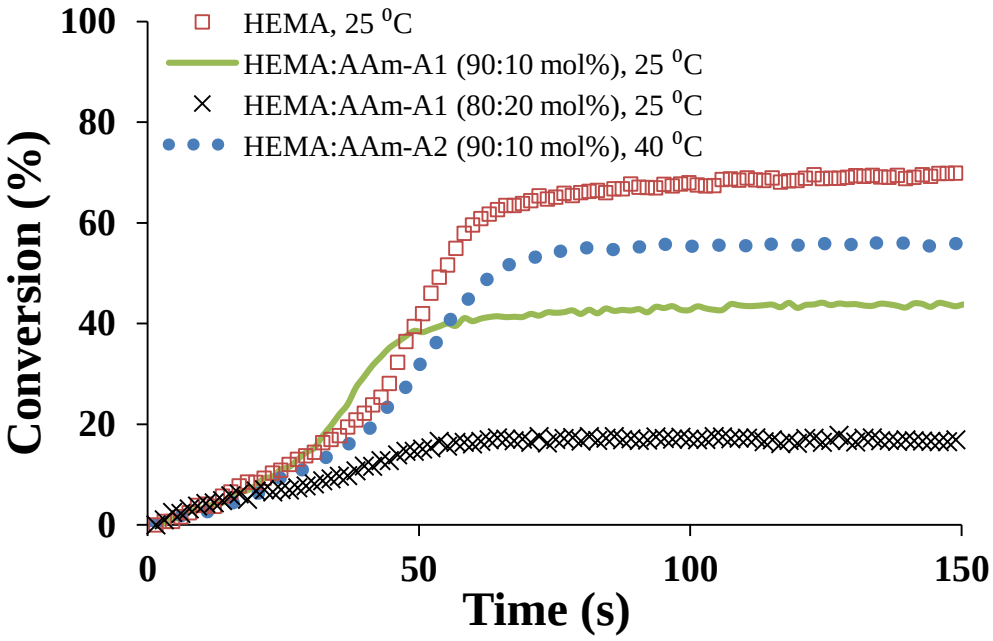

Figure 3.17. Conversion vs time plot of HEMA:AAm-A1 and HEMA:AAm-A2 mixtures at different temperatures

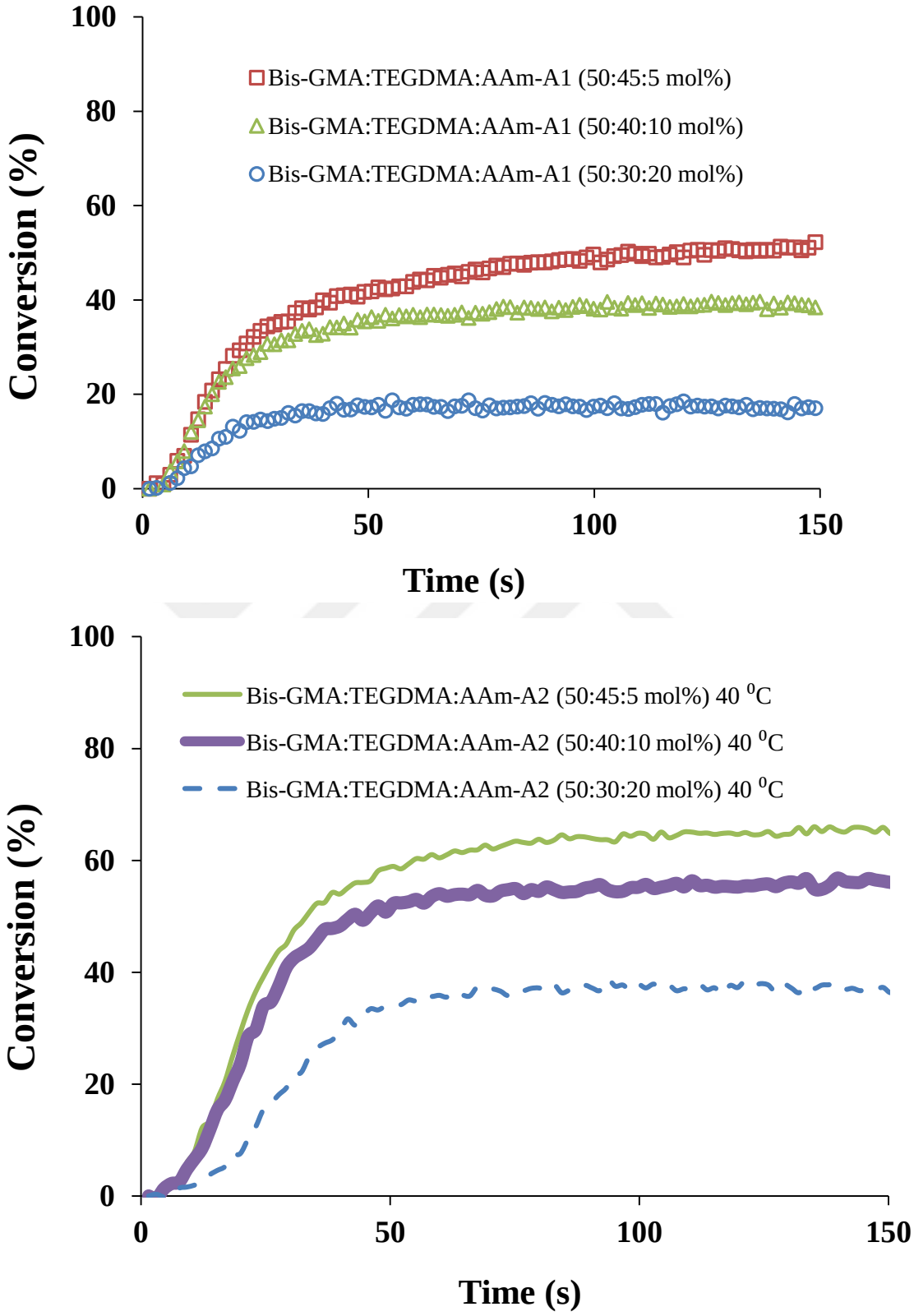

Figure 3.18. Conversion vs time plot of Bis-GMA:TEGDMA:AAm-A1 and Bis-GMA:TEGDMA:AAm-A2 mixtures at different temperatures

MA-A1 and MA-A2 were also copolymerized with HEMA at 37 °C by photo-DSC, using DMPA (2 mol%) as photoinitiator (Figure 3.21&3.22). It was observed that incorporation of MA-A1 or MA-A2 into HEMA reduced both the time (t_{max}) and conversions compared to HEMA depending on their concentrations in the formulations, while the maximum polymerization rates are similar. The low conversion values can be explained by the higher viscosity of MA-A1 and MA-A2 compared to HEMA, increasing viscosity of the resulting mixtures. The increased viscosity causes a decrease in the mobilities of reactive species and also leads to fast gelation of the mixture. However, Bis-GMA:TEGDMA:MA-A1/MA-A2 mixtures have higher polymerization yield than HEMA:MA-A1/MA-A2 mixtures owing to their higher polymerization rate. At high polymerization rates, the gelation cannot keep up with the fast polymerization and conversion is enhanced.

The copolymerization behaviours of acidic monomer (MA-A2-Ac) with HEMA, with HEMA:H_2O mixture, and with Bis-GMA:TEGDMA mixture were investigated by photo-DSC using BAPO (2 mol%) as photoinitiator at 37 °C. Rate vs time and conversion vs time plots are shown in Figure 3.23-3.26. Addition of MA-A2-Ac (10 mol%) to HEMA did not change R_{pmax} but decreased t_{max} and conversion values, compared to HEMA (Figure 3.23, 3.24). The low conversion values are probably due to the higher viscosity of MA-A2-Ac compared to HEMA, increasing viscosity of the formulation. The increased viscosity leads to early gelation of the mixture. MA-A2-Ac (10 mol%) addition to Bis-GMA:TEGDMA mixture didn't change t_{max} compared to Bis-GMA:TEGDMA mixture (Figure 3.23), but raised conversion to 83% (Figure 3.24). Again, replacement of difunctional monomer (TEGDMA) by a monofunctional monomer (MA-A2-Ac) causes this increase in conversion. HEMA:water:MA-A2-Ac mixture reached faster to max. polymerization rate than HEMA:water mixture as seen in rate plot (Figure 3.25). Its conversion value is very high (>100%) (Figure 3.26). This high value may be due to evaporation of water during photopolymerization.

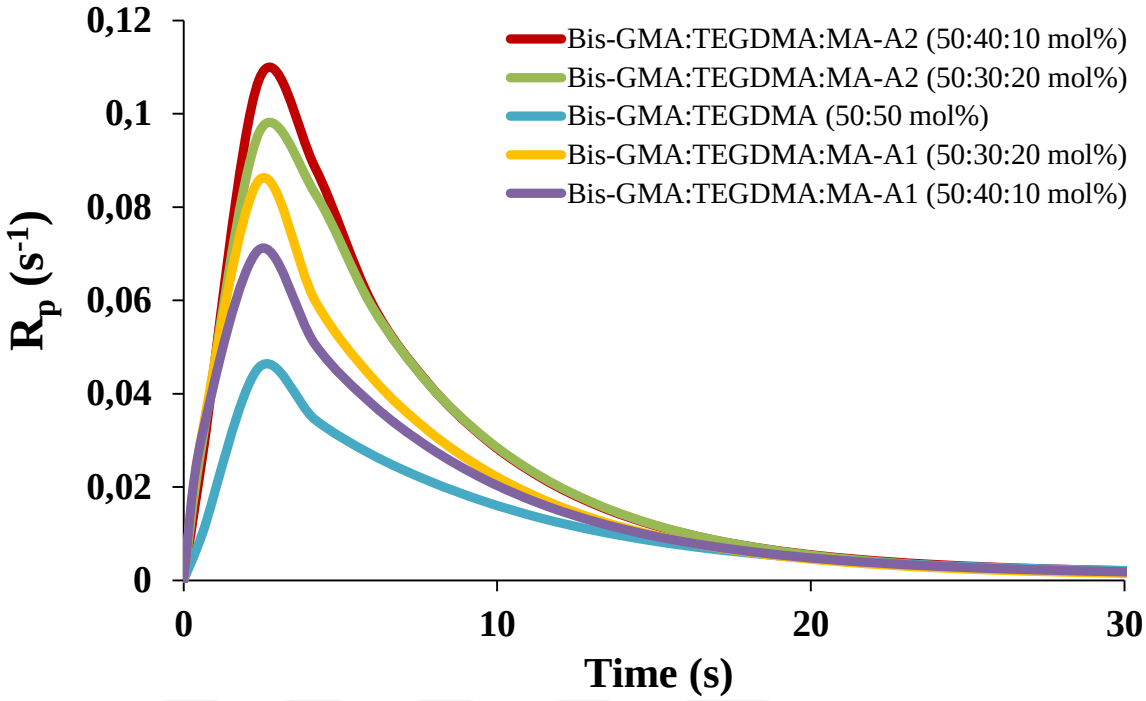

Figure 3.19. R_p vs time plot for Bis-GMA:TEGDMA:MA-A1/MA-A2 mixtures at 37°C

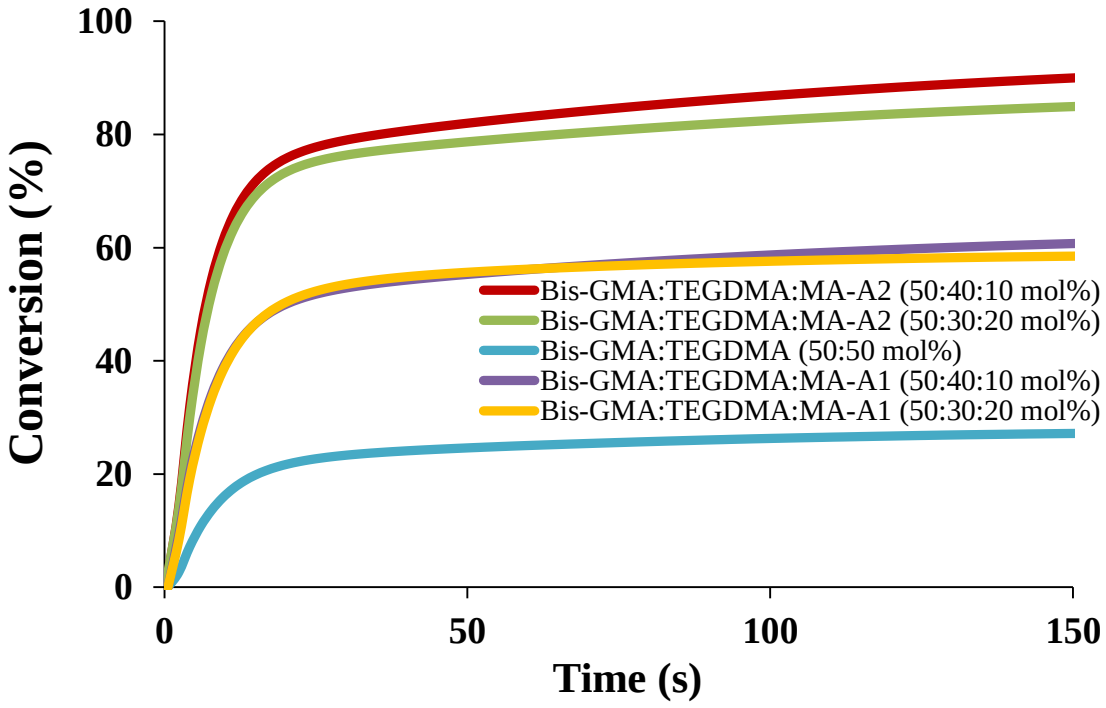

Figure 3.20. Conversion vs time plot for Bis-GMA:TEGDMA:MA-A1/MA-A2 mixtures at 37 °C

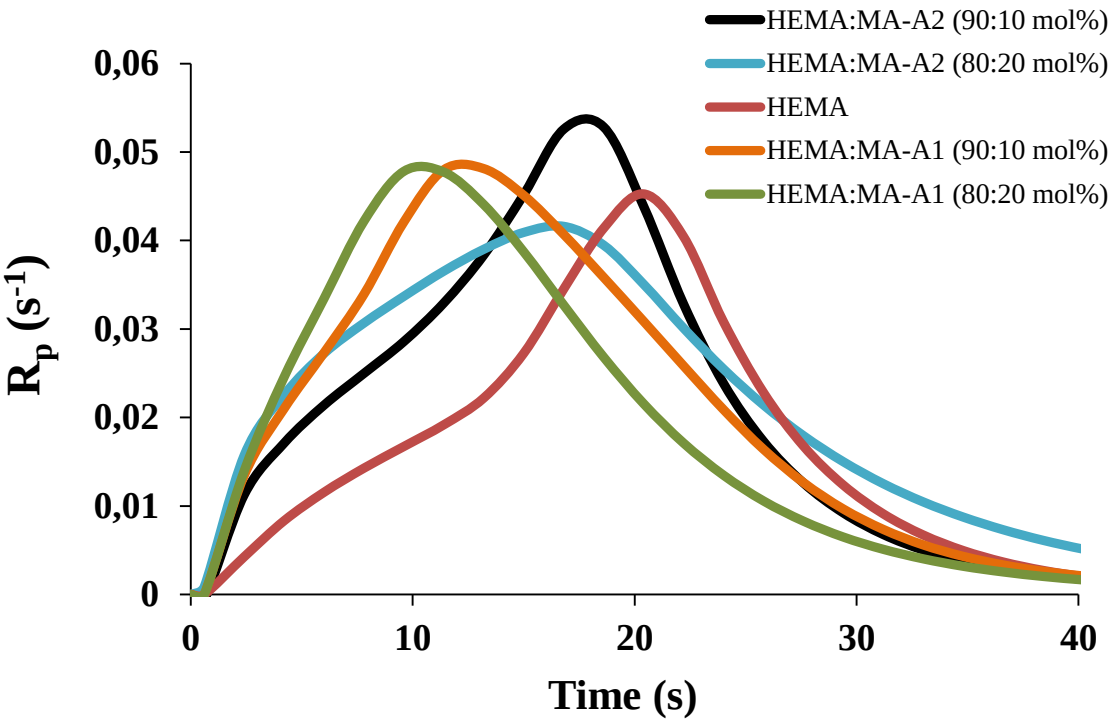

Figure 3.21. R_p vs time plot for HEMA:MA-A1/MA-A2 mixtures at 37 °C

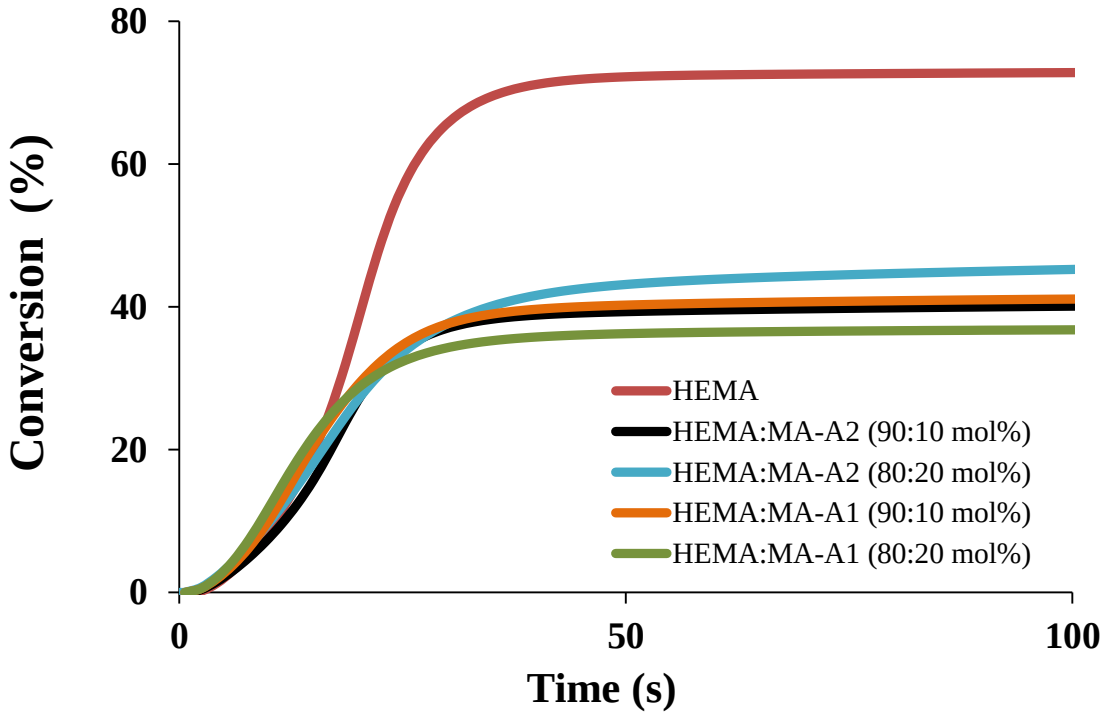

Figure 3.22. Conversion vs time plot for HEMA:MA-A1/MA-A2 mixtures at 37 °C

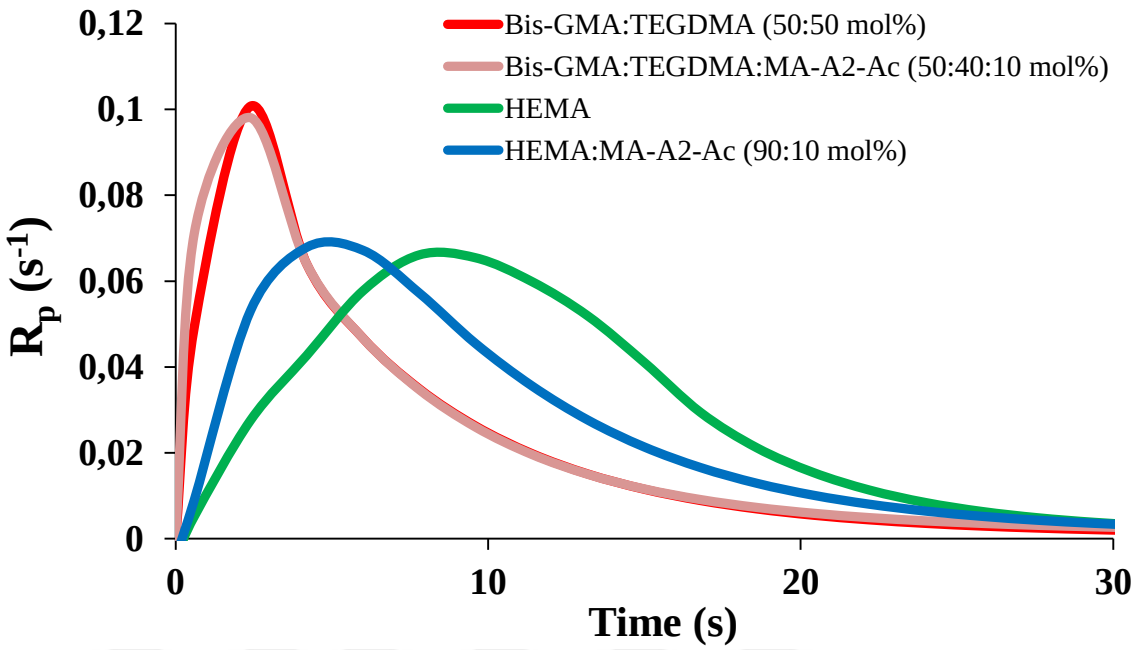

Figure 3.23. R_p vs time plot for HEMA, HEMA:MA-A2-Ac, Bis-GMA:TEGDMA, and Bis-GMA:TEGDMA:MA-A2-Ac mixtures at 37 °C (initiator: BAPO)

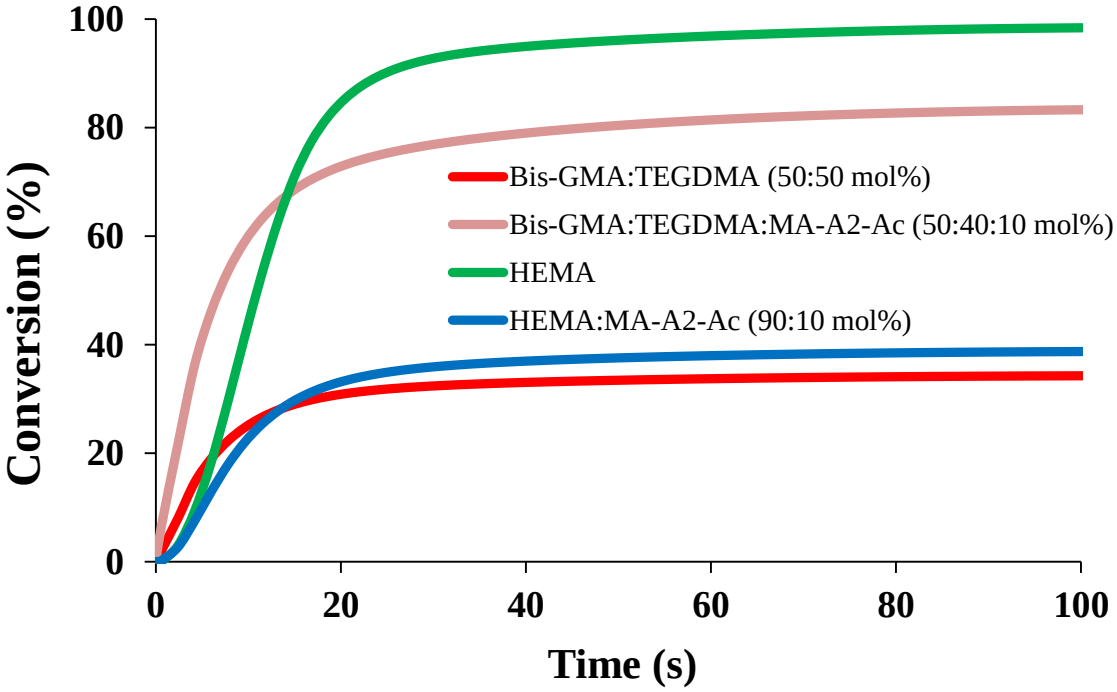

Figure 3.24. Conversion vs time plot for HEMA, HEMA:MA-A2-Ac, Bis-GMA:TEGDMA, and Bis-GMA:TEGDMA:MA-A2-Ac mixtures at 37 °C (initiator: BAPO)

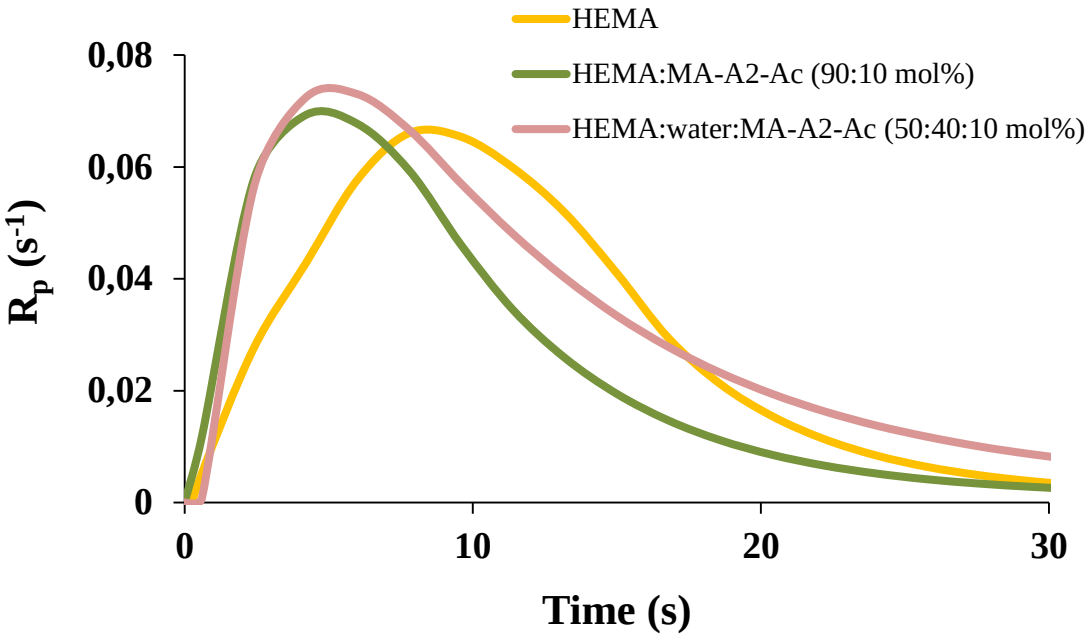

Figure 3.25. R_p vs time plot for HEMA, HEMA:MA-A2-Ac, and HEMA:water:MA-A2-Ac mixtures at 37 °C (initiator: BAPO)

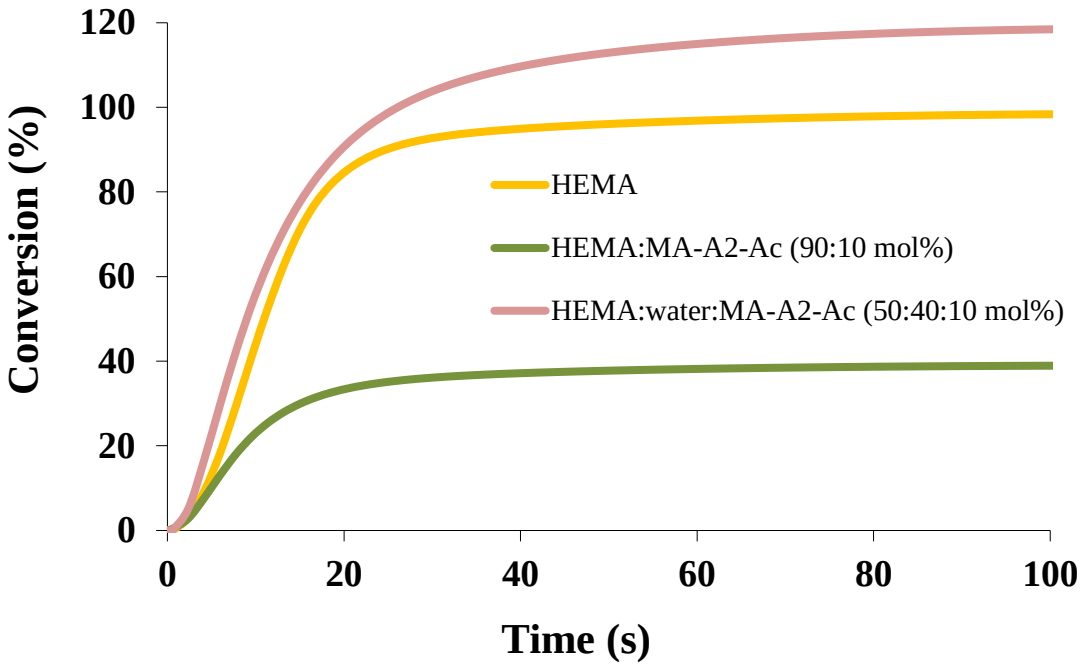

Figure 3.26. Conversion vs time plot for HEMA, HEMA:MA-A2-Ac, and HEMA:water:MA-A2-Ac mixtures at 37 °C (initiator: BAPO)

3.4. *In vitro* Cytotoxicity Assay

The cytotoxicity of the two methacylate monomers - MA-A2 and MA-A2-Ac (acidic) - were tested on NIH 3T3 mouse embryonic fibroblast cells using standart MTT assay. Materials resulting in more than 80% viability are defined as non-cytotoxic according to ISO 10993-5 [74]. Figure 3.27 indicates that no significant cytotoxicity was detected between 10-200 μg/mL in 24 h. Less than 80 % cell viability was only observed for 100 μg/mL of MA-A2, but it was caused by standard deviation. MA-A2 and MA-A2-Ac are non-toxic with the tested range.

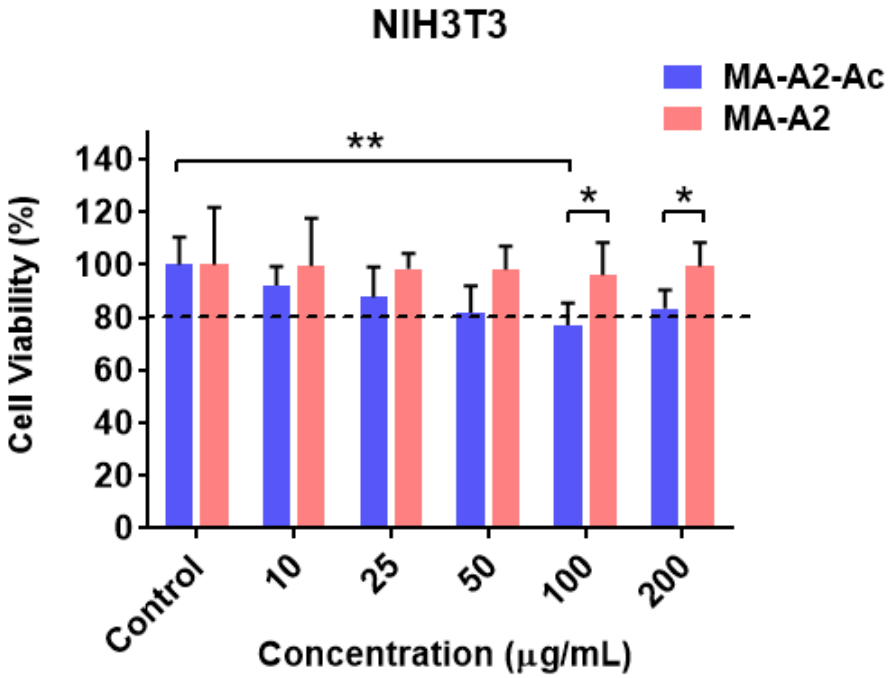

Figure 3.27. Cell viability plot of MA-A2 and MA-A2-Ac

3.5. Thermal Polymerization

Solution copolymerizations of AAm-A2 with PEGMA in two different feed ratios (50:50 and 20:80 mol%, AAm-A2:PEGMA) were carried out in methanol at 60 °C using AIBN. The soluble polymers were purified by precipitation into diethyl ether to obtain white solids after 2 h. Figure 3.28 shows the ^{1}H NMR spectrum of one of the copolymers

(AAm-A2:PEGMA, 50:50 mol% in feed). The peaks between 1.3-1.7 ppm correspond to methyl protons of PEGMA and AAm-A2, methylene protons adjacent to phosphorus, methylene protons on alkyl chain of AAm-A2, and copolymer backbone protons. The peaks at 3.35 and 3.6 ppm are due to methoxy (OCH_3) and methylene protons (OCH_2CH_2) of PEGMA. PEGMA methylene protons adjecent to ester oxygen and AAm-A2 methylene adjecent to phosphonate ester oxygen overlapped around 4.2 ppm. The methine proton of AAm-A2 was observed around 3.45 ppm. Integration of the peaks at 3.35 and 4.15 ppm were used to calculate the copolymer composition and gives AAm-A2:PEGMA as 30:70 (AAm-A2:PEGMA, 50:50 mol% in feed) and 6:94 (AAm-A2:PEGMA, 20:80 mol% in feed) mol % (Figure 3.29). In the FTIR spectra of the copolymer, P=O and P-O peaks confirm the incorporation of AAm-A2 to the copolymer (Figure 3.30).

The phosphonate ester groups of AAm-A2:PEGMA (20:80 mol% in feed) copolymer were deprotected by TMSBr. ^{1}H NMR spectrum of the copolymer proves the disappearance of methyl (1.2 ppm) and methylene (4.2 ppm) protons of phosphonate ester (Figure 3.31).

These copolymers may have potential to be used for two important areas: remineralization of demineralized dentin by forming composite with calcium phosphate nanoparticles and bone targeting polymers for biomedical applications. These topics will be studied.

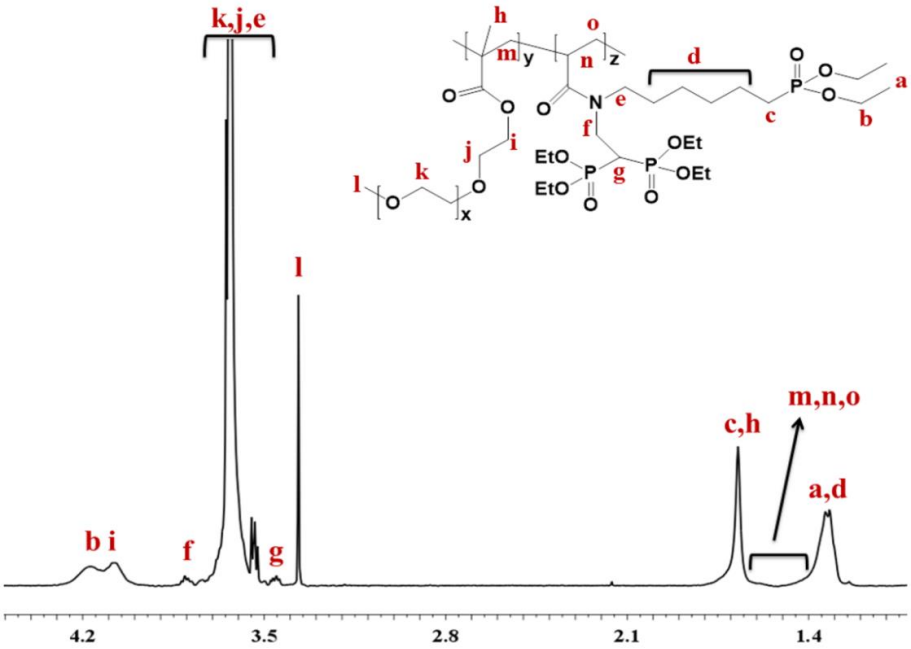

Figure 3.28. ^{1}H NMR spectrum of PEGMA:AAm-A2 (50:50 mol% in feed) copolymer

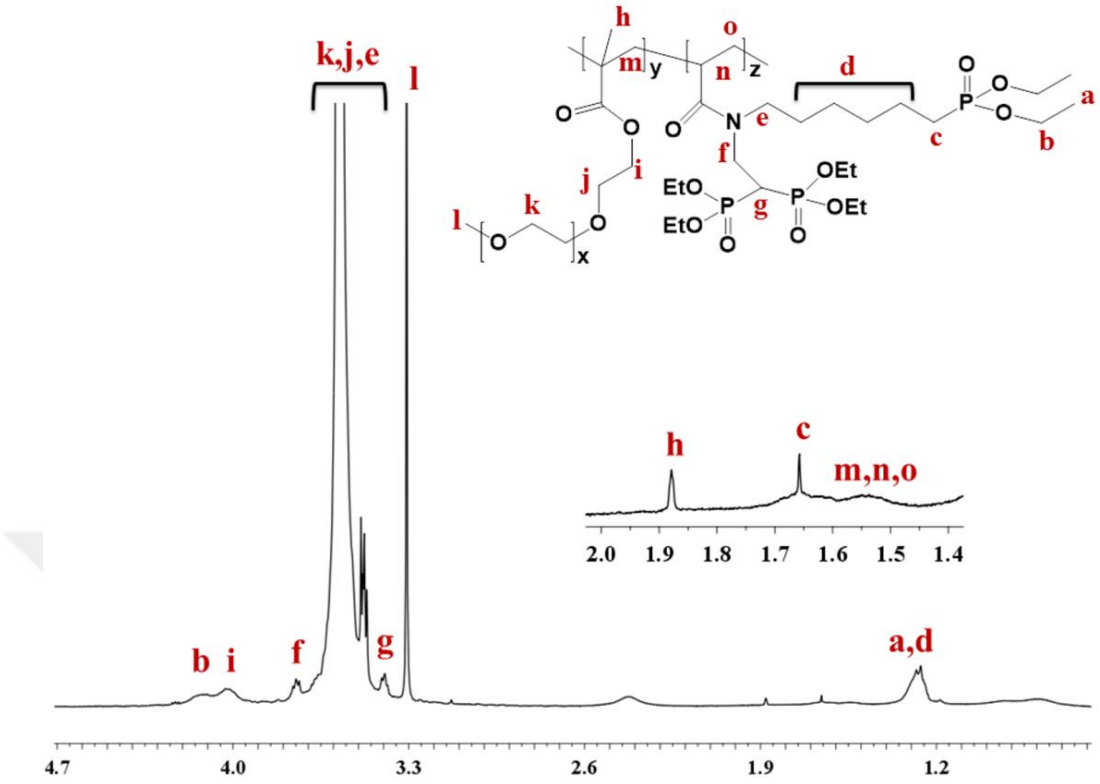

Figure 3.29. ^{1}H NMR spectrum of PEGMA:AAm-A2 (80:20 mol% in feed) copolymer

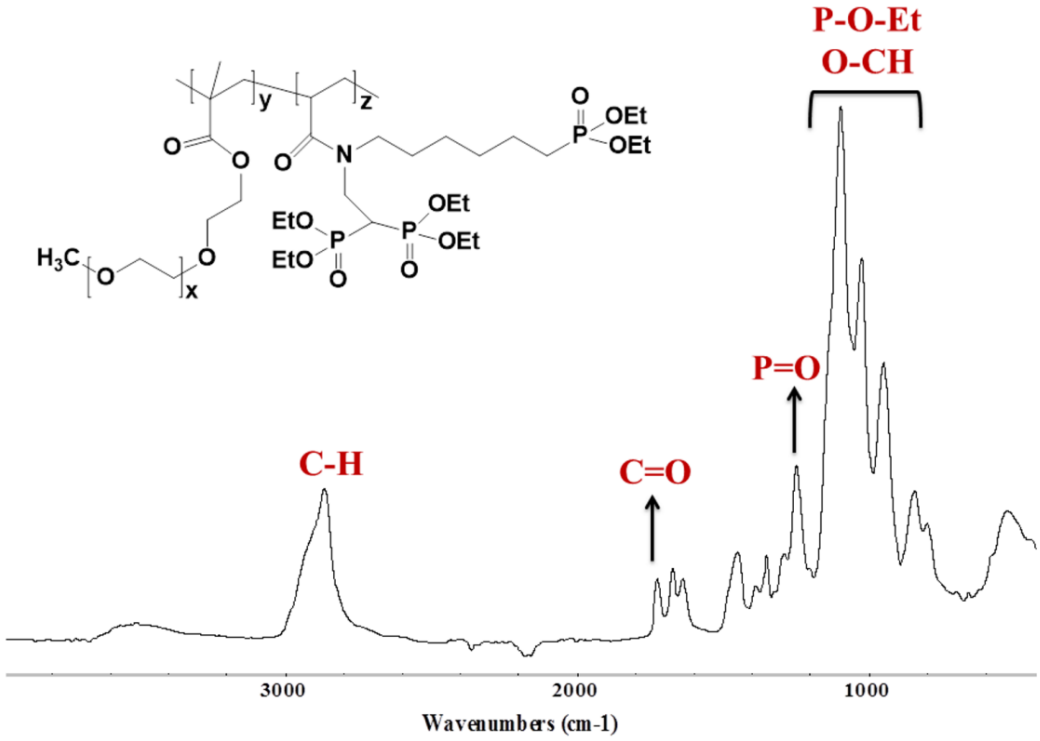

Figure 3.30. FTIR spectrum of PEGMA:AAm-A2 (80:20 mol% in feed) copolymer

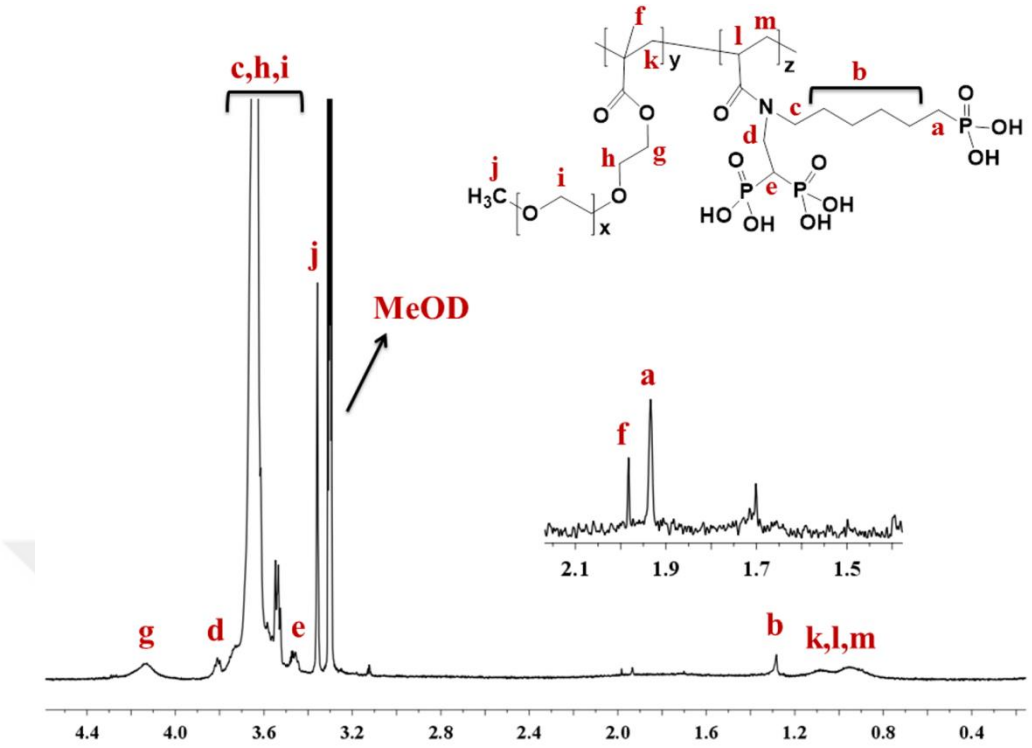

Figure 3.31. ^{1}H spectrum of deprotected PEGMA:AAm-A2 (80:20 mol% in feed) copolymer

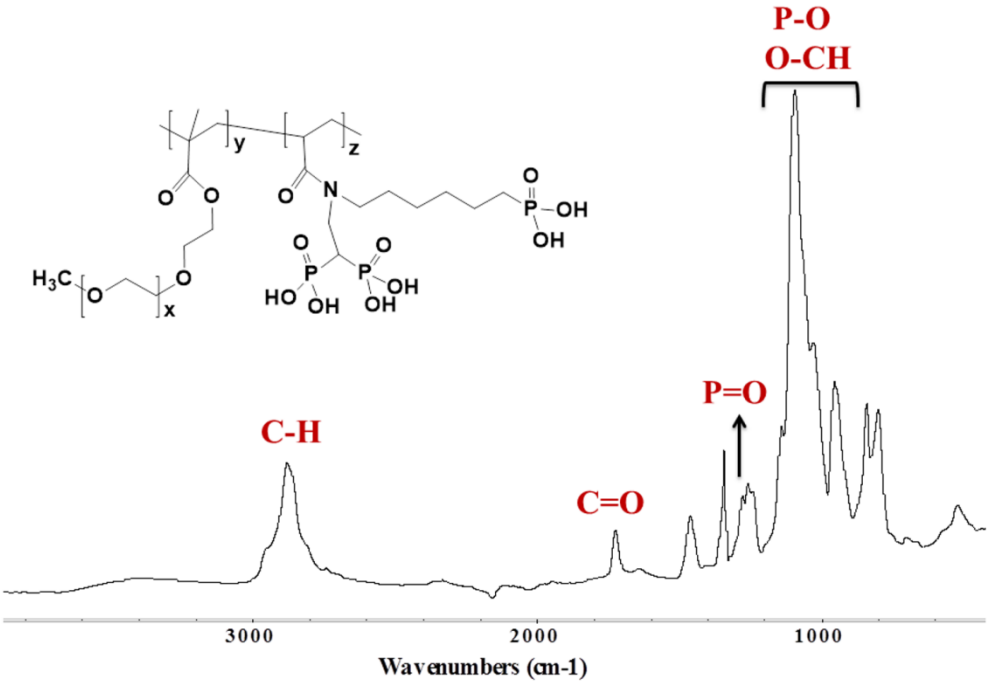

Figure 3.32. FTIR spectrum of deprotected PEGMA:AAm-A2 (80:20 mol% in feed) copolymer

Amine/Monomer	Petroleum Ether	Diehyl Ether	DCM	THF	MeOH	H_2O
A1	-	+	+	+	+	+
A2	-	+	+	+	+	+
AAm-A1	-	+	+	+	+	+
AAm-A2	-	+	+	+	+	+
MA-A1	-	+	+	+	+	+
MA-A2	-	+	+	+	+	+
MA-A1-Ac	-	-	-	-	+	+
MA-A2-Ac	-	-	-	-	+	+

Table 3.1. Solubilities of amines and monomers in different solvents

4. DISCUSSION&CONCLUSION

In this thesis, two novel amines containing both phosphonate and bisphosphonate groups (A1 and A2) were synthesized via Michael addition between tetraethyl vinylidene bisphosphonate and diethyl (2-aminoethyl) phosphonate or diethyl (6-aminohexyl) phosphonate. It is possible to use this metod to prepare amines with a range of hydrophilic/hydrophobic properties depending on the alkyl chain length.

A1 and A2 were reacted with acryloyl chloride to synthesize two novel water soluble acrylamide monomers (AAm-A1 and AAm-A2) containing both phosphonate and bisphosphonate functionalities. These monomers were copolymerized with commercial methacrylates used in dental composites (Bis-GMA/TEGDMA and HEMA) by real-time FTIR. The decrease both in polymerization rate and conversion with increasing fractions of AAm-A1 and AAm-A2 can be explained by the steric effect of the synthesized monomers. The dealkylation of the phosphonate/bisphosphonate ester groups in these monomers by TMSBr wasn't successful due to loss of the double bond after the reaction. However, the copolymerization of AAm-A2 with PEGMA (M_n = 950) in two different ratios (AAm-A2:PEGMA, 50:50 and 20:80 mol% in feed) followed by dealkylation of the phosphonate/bisphosphonate ester groups with TMSBr gave polymers with phosphonic and bisphosphonic acid functionalities. These acidic copolymers are considered to be good candidates for biomedical applications such as remineralization of demineralized dentin by forming composite with calcium phosphate nanoparticles and for bone targeting applications. Further investigations will be conducted.

A1 and A2 were also reacted with IEM to obtain two novel methacrylate monomers (MA-A1 and MA-A2) containing both phosphonate and bisphosphonate functionalities. These monomers were copolymerized with Bis-GMA:TEGDMA mixture to find out their potential use in dental composites. The high rate and conversion values can be explained by i) increased gelation time due to replacement of a difunctional monomer with a monofunctional one, so conversion is also raised; ii) hydrogen bonding due to urea groups, so both rate and conversion is increased. Based on the results, it can be deduced that MA-A1 and MA-A2 can be used as reactive diluent in Bis-GMA:TEGDMA mixture. However, addition of the synthesized monomers to HEMA decreased the conversion without a

significant change in rate of polymerization. Rigid and polar structures of the monomers in a more slow polymerizing system cause early gelation, and decrease conversion.

Phosphonate/bisphosphonate esters of MA-A1 and MA-A2 were dealkylated by TMSBr to obtain two novel methacrylate monomers having both phosphonic and bisphosphonic acid functionalities (MA-A1-Ac and MA-A2-Ac). These acidic monomers are water soluble which is essential for dental applications. The pH values of these monomers are 1.65 and 1.66 for MA-A1-Ac and MA-A2-Ac, respectively, in the range that qualifies them as mild self-etching adhesives. It has been proven by SEM analysis that MA-A2-Ac etches enamel and dentin, and removes smear layer partially. Interaction between HAP and this monomer was analyzed by FTIR, XPS and XRD. XPS was repeated for a commercial dental monomer (MDP) and results were compared. FTIR spectrum of MA-A2-Ac treated HAP shows a C=O peak, indicating incorporation of the monomer on HAP. XPS spectrum shows more intensified C1s (C-C, C-H, C=C) peak compared to HAP, and XRD plot proves presence of monomer-Ca salt. These analyses are indication of interaction between HAP and MA-A2-Ac, similar to MDP. HAP – MA-A2-Ac interaction is stronger than the interaction between HAP and only phosphonic acid containing monomers. MA-A1-Ac – HAP interaction will be analyzed with the same methods.

The acidic monomer (MA-A2-Ac) was copolymerized with HEMA in the presence of water using photo-DSC. HEMA:H_2O:monomer mixture showed similar polymerization rate and conversion with HEMA, proving that the acidic monomer is good candidate for dental adhesives. However, we were unable to replace the ester groups which can hydrolyze in acidic aqueous medium, possibly leading to short life time. Still these monomers will help improve new water-free dental adhesive systems.

In vitro cytotoxicity assay conducted for MA-A2 and MA-A2-Ac showed minimum cell viability of 80%, indicating that the synthesized monomers are not toxic.Because of standard deviation, 100 μg/ml of MA-A2-Ac showed cell viability lower than 80%. Overall, the synthesized novel methacrylate monomers are not toxic.

In conclusion, novel adhesive monomers are synthesized in this project. Monomers can bind strongly to tooth tissue (similar to MDP, one of the strongly binding monomers

known) when added to dental adhesive and composite mixtures. They also can be used as reactive diluents. Monomer structure – polymerization reactivity and tooth binding relations will be researched in more detail. The use of synthesized monomers in different biomedical applications will be examined.

5. REFERENCES

1. Banerjee S, Wehbi M, Manseri A, Mehdi A, Alaaeddine A, Hachem A, Ameduri B. Poly(vinylidene fluoride) Containing Phosphonic Acid as Anticorrosion Coating for Steel, *ACS Applied Mateials Interfaces*, 2017, *9*, 6433−6443.

2. David G, Ortega E, Chougrani K, Manseri A, Boutevin B. Grafting of phosphonate groups onto PVA by acetalyzation. Evaluation of the anti-corrosive properties for the acetalyzed PVA coatings, *Reactive & Functional Polymers*, 2011, 71, 599–606.

3. Lu Y, Zhang Z, Li Y, Li W. Extraction and recovery of cerium(IV) and thorium(IV) from sulphate medium by an α-aminophosphonate extractant, *Journal of Rare Earths*, 2017, *35*, 34 – 40.

4. Chouyyok W, Pittman JW, Warner MG, Nell KM, Clubb DC, Gillc GA, Addleman RS. Surface functionalized nanostructured ceramic sorbents for the effective collection and recovery of uranium from seawater, *Dalton Transactions*, 2016, *45*, 11312–1132.

5. Ali SA, Kazi IW, Ullah N. New Chelating Ion-Exchange Resin Synthesized via the Cyclopolymerization Protocol and Its Uptake Performance for Metal Ion Removal, *Industrial & Engineering Chemistry Research*, 2015, *54*, 9689−9698.

6. Silbernagel R, Martin CH, Clearfield A. Zirconium(IV) Phosphonate−Phosphates as Efficient Ion-Exchange Materials, *Inorganic Chemistry*, 2016, *55*, 1651−1656.

7. Awual MdR, Shenashen MA, Yaita T, Shiwaku H, Jyo A. Efficient arsenic(V) removal from water by ligand exchange fibrous adsorbent, *Water Research*, 2012, *46*, 5541 – 5550.

8. Graillot A, Bouyer D, Monge S, Robin J-J, Faur C. Removal of nickel ions from aqueous solution by low energy-consuming sorption process involving thermosensitive copolymers with phosphonic acid groups, *Journal of Hazardous Materials*, 2013, *244–245*, 507– 515.

9. Majka TM, Leszczyńska A, Kandola BK, Pornwannachai W, Pielichowski K. Modification of organo-montmorillonite with disodium H-phosphonate to develop flame retarded polyamide 6 nanocomposites, *Applied Clay Science*, 2017, *139*, 28–39.

10. Xiang HF, Xu HY, Wang ZZ, Chen CH. Dimethyl methylphosphonate (DMMP) as an efficient flame retardant additive for the lithium-ion battery electrolytes, *Journal of Power Sources*, 2007, *173*, 562–564.

11. Berts I, Ossipov D, Fragneto G, Frisk A, Rennie AD. Polymeric Smart Coating Strategy for Titanium Implants, *Advanced Engineering Materials*, 2014, *16*, 1340-1350.

12. Auernheimer J, Zukowski D, Dahmen C, Kantlehner M, Enderle A, Goodman SL, Kessler H. Titanium Implant Materials with Improved Biocompatibility through Coating with Phosphonate-Anchored Cyclic RGD Peptides, *ChemBioChem*, 2005, *6*, 2034 – 2040.

13. Meng H, Liong M, Xia T, Li Z, Ji Z, Zink JI, Nel AE. Engineered Design of Mesoporous Silica Nanoparticles to Deliver Doxorubicin and P-Glycoprotein siRNA to Overcome Drug Resistance in a Cancer Cell Line, *ACS Nano*, 2010, *4*, 4539–4550.

14. Hałupka-Bryl M, Asai K, Thangavel S, Bednarowicz M, Krzyminiewski R, Nagasaki Y. Synthesis and in vitro and in vivo evaluations of poly(ethyleneglycol)-block-poly(4-vinylbenzylphosphonate) magneticnanoparticles containing doxorubicin as a potential targeted drug delivery system, *Colloids and Surfaces B*, 2014, *118*,140–147.

15. Catel Y, Bock T, Moszner N. Monomers for Adhesive Polymers. XV. Synthesis, Photopolymerization, and Adhesive Properties of Polymerizable b-Ketophosphonic Acids, *Journal of Poymer Science Part:A: Polymer Chemistry*, 2014, *52*, 3550-3563.

16. Van Landuyt KL, Snauwaert J, De Munck J, Peumans M, Yoshida Y, Poitevin A, Coutinho E, Suzuki K, Lambrechts P, Van Meerbeek B. Systematic review of the chemical composition of contemporary dental adhesives, *Biomaterials*, 2007, *28*, 3757–3785.

17. Buonocore MG. A Simple Method of Increasing The Adhesıon of Acrylic Filling Materials to Enamel Surfaces, *Journal of Dental Research*, 1955, 34, 849 – 853.

18. Moszner N, Salz U, Ziemmermann J. Chemical Aspects of Self-etching Enamel–dentin Adhesives: A systematic Review, *Dental Materials*, 2005, *21*, 895-910.

19. Moszner N, Salz U. Recent Developments of New Components for Dental Adhesives and Composites, *Macromolecular Materials and Engineering*, 2007, *292*, 245-271.

20. Moszner N, Hirt T. New Polymer-Chemical Developments in Clinical Dental Polymer Materials: Enamel-Dentin Adhesives and Restorative Composites, *Journal of Polymer Science Part A: Polymer Chemistry*, 2012, *50*, 4369-4402.

21. Ferracane JL, Stansbury JW, Burke FJT. Self-adhesive Resin Cements-chemistry, Properties and Clinical Considerations, *Journal of Oral Rehabilitation*, 2011, *38*, 295-314.

22. Van Meerbeek B, Yoshihara K, Yoshida Y, Mine A, De Munck J, Van Landuyt KL. State of the Art of Self-etch Adhesives, *Dental Materials*, 2011, *27*, 17–28.

23. Yoshida Y, Van Meerbeek B, Nakayama Y, Yoshioka M, Snauwaert J, Abe Y, Lambrechts P, Vanherle G, Okazaki M. Adhesion to and Decalcification of Hydroxyapatite by Carboxylic Acids, *Journal of Dental Research*, 2001, *80*, 1565-1569.

24. Feitosa VP, Ogliari FA, Van Meerbeek B., Watson TF, Yoshihara K., Ogliari AO, Sinhoreti MA, Correr AB, Cama G, Sauro S. Can the Hydrophilicity of Functional Monomers Affect Chemical Interaction?, *Journal of Dental Research*, 2014, *93*, 201-206.

25. Ikemura K, Tay FR, Nishiyama N, Pashley D, Endo T. Design of New Phosphonic Acid Monomers for Dental Adhesives - Synthesis of (Meth)acryloxyalkyl 3-Phosphonopropionates and Evaluation of Their Adhesion-promoting Functions, *Dental Materials Journal*, 2006, *25*, 566-575.

26. Inoue S, Koshiro K, Yoshida Y, De Munck J, Nagakane K, Suzuki K, Sano H, Van Meerbeek B. Hydrolytic Stability of Self-etch Adhesives Bonded to Dentin, *Journal of Dental Research*, 2005, *84*, 1160-1164.

27. Van Landuyt KL, Yoshida Y, Hirata I, Snauwaert J, De Munck J, Okazaki M, Suzuki K, Lambrechts P, Van Meerbeek B. Influence of the Chemical Structure of Functional

Monomers on Their Adhesive Performance, *Journal of Dental Research*, 2008, *87*, 757-761.

28. Nakabayashi N, Kojima K, Masuhara E. The promotion of adhesion by the infiltration of monomers into tooth substrates, *Journal of Biomedical Materials Research*, 1982, *16*, 265-273.

29. Moszner N, Salz U, Zimmermann J. Chemical aspects of self-etching enamel–dentin adhesives: A systematic review, *Dental Materials*, 2005, *21*, 895–910.

30. Yoshida Y, Nagakane K, Fukuda R, Nakayama Y, Okazaki M, Shintani H, Inoue S, Tagawa Y, Suzuki K, De Munck J, Van Meerbeek B. Comparative Study on Adhesive Performance of Functional Monomers, *Journal of Dental Research*, 2004, *83*, 454-458.

31. Yoshida Y, Inoue S. Chemical analyses in dental adhesive technology, *Japanese Dental Science Review*, 2012, *48*, 141—152.

32. Albayrak AZ, Saraylı Z, Avcı D. Influence of Structure on Polymerization Rates and Ca-Binding of Phosphorus-Containing 1,6-Dienes, *Macromolecular Reaction Engineering*, 2007, *1*, 537-546.

33. Altin A, Akgun B, Sarayli Bilgici Z, Turker SB, Avci D. Synthesis, Photopolymerization, and Adhesive Properties of Hydrolytically Stable Phosphonic Acid-containing (Meth)acrylamides, *Journal of Polymer Science Part A: Polymer Chemistry*, 2014, *52*, 511-522.

34. Avci D, Mathias LJ. Synthesis and Polymerization of Phosphorus-containing Acrylates, *Journal of Polymer Science Part A: Polymer Chemistry*, 2002, *40*, 3221-3231.

35. Catel Y, Fischer UK, Moszner N. Monomers for Adhesive Polymers, 10-Synthesis, Radical Photopolymerization and Adhesive Properties of Methacrylates Bearing Phosphonic Acid Groups, *Macromolecular Materials Engineering*, 2013, *298*, 740–756.

36. Catel Y, Degrange M, Pluart LL, Madec P, Pham T, Picton L. Synthesis, Photopolymerization and Adhesive Properties of New Hydrolytically Stable

Phosphonic Acids for Dental Applications, *Journal of Polymer Science Part A: Polymer Chemistry*, 2008, *46*, 7074-7090.

37. Hino K, Yamauchi J, Nishida K. *Dental Compositions*, 1994, Kuraray Co., Ltd., US 5 321 053.

38. Klee JE, Walz U. Hydrolysis Stable One-part Self-etching, Self-priming Dental Adhesive, 2004 Dentsply DeTrey GmbH, US 6 812 266 B2.

39. Klee, JE, Lehmann U. N-alkyl-N-(phosphonoethyl) Substituted (Meth)acrylamides– New Adhesive Monomers for Self-etching Self-priming one Part Dental Adhesive, *Beilstein Journal of Organic Chemistry*, 2009, *5*, 1-9.

40. Mou L, Singh G, Nicholson JW. Synthesis of a Hydrophilic Phosphonic Acid Monomer for Dental Materials, *Chemical Communications*, 2000, 345-346.

41. Moszner N, Zeuner F, Fischer UK, Rheinberger V. Monomers for Adhesive Polymers, 2. Synthesis and Radical Polymerization of Hydrolytically Stable Acrylic Phosphonic Acids, *Macromolecular Chemistry and Physics*, 1999, *200*, 1062-1067.

42. Moszner N, Zeuner F, Pfeiffer S, Schurte I, Rheinberger V, Drache M. Monomers for Adhesive Polymers, 3. Synthesis, Radical Polymerization and Adhesive Properties of Hydrolytically Stable Phosphonic Acid Monomers, *Macromolecular Materials and Engineering*, 2001, *286*, 225-231.

43. Moszner N, Salz U, Zeuner F, Zimmermann J, Rheinberger V, Angermann J, Fischer UK. Dental Materials based on Acrylic-ester Phosphonic Acids, 2005, Ivoclar Vivadent US 6,900,251 B2.

44. Moszner N, Pavlinec J, Lamparth I, Zeuner F, Angermann J. Monomers for Adhesive Polymers, 6. Synthesis and Radical Polymerisation of 1,3-bis(Methacrylamido)propane-2-yl dihydrogen Phosphate, *Macromolecular Rapid Communications*, 2006, *27*, 1115-1120.

45. Omura I, Yamauchi J, Nagase Y, Uemura F. Phosphate Monoester Adhesive Composition, 1986, Kuraray Co., Ltd., US 4 612 384.

46. Omura I, Yamauchi J, Nagase Y, Uemura F. Adhesive Composition, 1987, Kuraray Co., Ltd. 4,650,847.

47. Pavlinec J, Zeuner F, Angermann J, Moszner N. Monomers for Adhesive Polymers, 5 Synthesis and Radical Polymerization Behavior of 2,4,6-Trimethylphenyl 2-[4-(dihydroxyphosphoryl)- 2-oxa-butyl]acrylate, *Macromolecular Chemistry and Physics*, 2005, *206*, 1878-1886.

48. Sahin G, Albayrak AZ, Bilgici ZS, Avci D. Synthesis and Evaluation of New Dental Monomers with Both Phosphonic and Carboxylic Acid Functional Groups, *Journal of Polymer Science Part A: Polymer Chemistry*, 2009**,** *47*, 1953-1965.

49. Salman S, Albayrak AZ, Avcı D, Aviyente V. Synthesis and Modeling of New Phosphorus-containing Acrylates, *Journal of Polymer Science Part A: Polymer Chemistry*, 2005, *43*, 2574-2583.

50. Senhaji O, Monge S, Chougrani K, Robin J-J. Synthesis, Characterization, and Photopolymerization of Novel Phosphonated Resins, *Macromolecular Chemistry and Physics*, 2008, *209*, 1694-1704.

51. Xu X, Wang R, Ling L, Burgess JO. Synthesis and Stability Study of Dental Monomers Containing Methacrylamidoethyl Phosphonic Acids, *Journal of Polymer Science Part A: Polymer Chemistry*, 2007, *45*, 99-110.

52. Yoshihara K, Yoshida Y, Hayakawa S, Nagaoka N, Torii Y, Osaka A, Suzuki K, Minagi S, Van Meerbeek B, Van Landuyt KL.Self-etch Monomer-Calcium Salt Deposition on Dentin, *Journal of Dental Research*, 2011, *90*, 602-606.

53. Catel Y, Dellsperger C, Moszner N. Monomers for adhesive polymers, 18. Synthesis, photopolymerization and adhesive properties of polymerizable α-phosphonooxy phosphonic acids, *Designed Monomers and Polymers*, 2017, *20*, 106-117.

54. Catel Y, Fischer UK, Moszner N. Monomers for adhesive polymers: 11. Structure–adhesive properties relationships of new hydrolytically stable acidic monomers, *Polymer International*, 2013, *62*, 1717–1728.

55. Derbanne MA, Besse V, Le Goff S, Sadoun M, Pham T-N. Hydrolytically stable acidic monomers used in two steps self-etch adhesives, *Polymer Degradation and Stability*, 2013, *98*, 1688 – 1698.

56. Besse V, Le Pluart L, Cook WD, Pham T-N, Madec P-J. Synthesis and Polymerization Kinetics of Acrylamide Phosphonic Acids and Esters as New Dentine Adhesives, *Journal of Polymer Science Part A: Polymer Chemistry*, 2013, *51*, 149–157.

57. Lourwood D. The Pharmacology and Therapeutic Utility of Bisphosphonates, *Pharmacotheraphy*, 1998, *18*, 779-89.

58. Page PCB, Moore JPG, Mansfield I, McKenzie MJ, Bowler WB, and Gallagher JA. Synthesis of Bone-Targeted Oestrogenic Compounds for The Inhibition of Bone Resorption, *Tetrahedron*, 2001, *57*, 1837-1847.

59. Wang JB, Yang CH, Yan XM, Wu XH, Xie YY. Novel Bone-targeted Agents for Treatment of Osteoporosis, *Chinese Chemical Letters*, 2005, *16*, 859-862.

60. Zhang S, Gangal G, Uludag H. Magic Bullets for Bone Diseases: Progress in Rational Design of Bone-seeking Medicinal Agents, *Chemical Society Reviews*, 2007, *36*, 507-531.

61. Abuelyaman AS, Boardman GS, Shukla BA, Aasen SM, Mitra SB, Mikulla M, Cinader DK. Compositions Including Polymerizable Bisphosphonic Acids and Methods, 2013, 3M Innovative Properties Co; US 8,404,144 B2.

62. Bala JL, Kashemirov BA, McKenna CE. Synthesis of a Novel Bisphosphonic Acid Alkene Monomer, *Synthetic Communications*, 2010, *40*, 3577–3584.

63. Catel Y, Degrange M, Le Pluart L, Madec PJ, Pham TN,Chen F, Cook WD.Synthesis, Photopolymerization, and Adhesive Properties of New Bisphosphonic Acid Monomers for Dental Application, *Journal of Polymer Science: Part A: Polymer Chemistry*, 2009, *47*, 5258-5271.

64. Catel Y, Besse V, Zulauf A, Marchat D, Pfund E, Pham T-N, Bernache-Assolant D, Degrange M, Lequeux T, Madec P-J, Le Pluart L. Synthesis and Evaluation of New Phosphonic, Bisphosphonic and Difluoromethylphosphonic Acid Monomers for Dental Application, *European Polymer Journal*, 2012, *48*, 318-330.

65. Moszner N, Catel Y, Angermann J, Bock T, Rheinberger V. Dental Materials on the Basis of Highly Acidic Polymerizable Bisphosphonic Acids, 2014, US 0296364 A1.

66. Akgun B, Avci D. Synthesis and Evaluations of Bisphosphonate-containing Monomers for Dental Materials, *Journal of Polymer Science: Part A: Polymer Chemistry*, 2012, *50*, 4854-4863.

67. Sarayli Bilgici Z, Turker SB, Avci D. Novel Bisphosphonated Methacrylates: Synthesis, Polymerizations, and Interactions with Hydroxyapatite, *Macromolecular Chemistry and Physics*, 2013, *214*, 2324-2335.

68. Rosowsky A, Forsch RA, Moran RG, Kohler W, Freisheim JH. Methotrexate Analog. 32. Chain Extension, .alpha.-carboxyl Deletion, and .gamma. Carboxyl Replacement by Sulfonate and Phosphate. Effect on enzyme Binding and Cell-growth Inhibition, *Journal of Medicinal Chemistry*, 1988, *31*, 1326-1331.

69. Shinkai S, Ishihara M, Ueda K, Manabe O. Photoresponsive Crown Ethers. Part 14. Photoregulated Crown-Metal Complexation by Competitive Intramolecular Tail(Ammonium)-biting, *Journal of Chemical Society Perkin Transactions*, 1985, *2*, 511-518.

70. Bako P, Novak T, Ludanyi K, Pete B, Toke L, Keglevich, G. D-Glucose-based Azacrown Ethers with a Phosphonoalkyl Side Chain: Application as Enantioselective Phase Transfer Catalysts, *Tetrahedon : Asymmetry*, 1999, *10*, 2373-2380.

71. Gali H, Prabhu KR, Karra SR, Katti KV. Facile Ring-Opening Reactions of Phthalimides as a New Strategy to Synthesize Amide-Functionalized Phosphonates, Primary Phosphines, and Bisphosphines, *Journal of Organic Chemistry*, 2000, *65*, 676–680.

72. Degenhardt CR, Burdsall DC. Synthesis of Ethenylidenebis(phosphonic acid) and Its Tetraalkyl Esters, *Journal of Organic Chemistry*, 1986, *51*, 3488-3490.

73. Yoshihara K, Yoshida Y, Hayakawa S, Nagaoka N, Torii Y, Osaka A, Suzuki K, Minagi S, Van Meerbeek B, Van Landuyt KL. Self-etch Monomer-Calcium Salt Deposition on Dentin, *Journal of Dental Research*, 2011, *90*, 602-606.

74. López-García J, Lehocký M, Humpolíček P, Sáha P. HaCaT Keratinocytes Response On Antimicrobial Atelocollagen Substrates: Extent Of Cytotoxicity, Cell Viability And Proliferation, *Journal of Functional Biomaterials*, 2014, *5*, 43–57.